



HAL
open science

Provenance of sculptural limestones in protohistoric Provence (SE France): Insights from carbonate rock petrography and stable isotope geochemistry

François Fournier, Adam Ouass, Pierre Rochette, Philippe Bromblet, Philippe Léonide, Gilles Conesa, Lionel Marié, Sarah Boularand, Anne-Marie d'Ovidio, Béatrice Vigié, et al.

► To cite this version:

François Fournier, Adam Ouass, Pierre Rochette, Philippe Bromblet, Philippe Léonide, et al.. Provenance of sculptural limestones in protohistoric Provence (SE France): Insights from carbonate rock petrography and stable isotope geochemistry. *Journal of Archaeological Science: Reports*, 2023, 48, pp.103922. <10.1016/j.jasrep.2023.103922>. <hal-04692586>

HAL Id: hal-04692586

<https://hal.science/hal-04692586v1>

Submitted on 27 Nov 2024

HAL is a multi-disciplinary open access archive for the deposit and dissemination of scientific research documents, whether they are published or not. The documents may come from teaching and research institutions in France or abroad, or from public or private research centers.

L'archive ouverte pluridisciplinaire HAL, est destinée au dépôt et à la diffusion de documents scientifiques de niveau recherche, publiés ou non, émanant des établissements d'enseignement et de recherche français ou étrangers, des laboratoires publics ou privés.



HAL Authorization

1 **Fournier, F., Ouass, A., Rochette, P., Bromblet, P., Léonide, P., Conesa, G., Marié, L., Boularand, S.,**
2 **D’Ovidio, A.-M., Vigie, B., Del Furia, L., Lemke, A.L., Niaissa, T., Tendil, A., Fleury J., 2023. Provenance**
3 **of sculptural limestones in protohistoric Provence (SE France): insights from carbonate rock**
4 **petrography and stable isotope geochemistry. *Journal of Archaeological Science : Reports*, 48, 103922.**

5
6
7 **Provenance of sculptural limestones in protohistoric Provence**
8 **(SE France): insights from carbonate rock petrography and stable isotope**
9 **geochemistry**

10
11 **Fournier, F.^{1,*}, Ouass, A.¹, Rochette, P.¹, Bromblet, P.², Léonide, P.¹, Conesa, G.¹,**
12 **Marié, L.¹, Boularand, S.³, D’Ovidio, A.-M.⁴, Vigie, B.⁵, Del Furia, L.⁶, Lemke¹, A.L.,**
13 **Niaissa, T.¹, Tendil, A.¹, Fleury J.¹**

14 ¹ Aix Marseille Univ, CNRS, IRD, Coll France, CEREGE, Technopôle de l’Arbois-Méditerranée, BP80, 13545
15 Aix-en-Provence, France.

16 ² CICRP (Centre Interdisciplinaire de Conservation et de Restauration du Patrimoine), 21 rue Guibal – 13003
17 Marseille

18 ³ Fédération de Recherche Sciences Chimiques Marseille FR 1739, Pôle PRATIM, 13331 Marseille Cedex 03,
19 France.

20 ⁴ Musée d’Histoire de Marseille, Pôle Archéologie – Ville de Marseille- Dépôt archéologique municipal, 146 av.
21 Roger Salengro 13233 Marseille Cedex 20

22 ⁵ Musée d’Histoire de Marseille – Ville de Marseille - Immeuble CMCI - 2, rue Henri-Barbusse, 13233 Marseille
23 Cedex 20

24 ⁶ Musée Ziem - 9, Boulevard du 14 juillet, 13500 Martigues

25 *Corresponding author: fournier@cerege.fr

26
27 **Abstract**

28
29 The combination of a detailed analysis of microfacies, diagenetic features and isotopic
30 signatures (carbon and oxygen) of limestones from protohistoric statues and the comparison
31 with substantial regional petrographic and geochemical databases have proven to be successful
32 for constraining the provenance and providing insights into the production of statuary materials
33 in Provence during the Iron Age. The limestones forming the sculptures from Roquepertuse

34 (*twin-headed "Hermes", the lintel with horses and the warrior seated cross-legged*) and
35 Rognac (*warrior seated cross-legged*) are interpreted to derive from lower Barremian carbonate
36 formations from La Fare Massif, likely from the vicinity of Coudoux, based on an analogy in
37 1) micropalaeontologic markers (orbitolinids), 2) grain size, texture and grain composition
38 (oolithic, oobioclastic and bioclastic grainstones), 3) dissolution features affecting ooid cortices
39 and 4) carbon and oxygen isotope signatures. The bryozoan-echinoderm association and the
40 occurrence of *Amphistegina* suggest that the *bust of warrior* from La Cloche oppidum is made
41 of a Miocene limestone from La Couronne formation. Its isotope composition suggests a
42 provenance from quarries located at Anse du Verdon or possibly further to the west. This
43 demonstrates a use of La Couronne limestone as a statuary material in protohistoric times (3rd
44 to 1st century BC). The *fragment of scapulary tunic* found in a disturbed archaeological context
45 dated of 6th to 2nd century BC on the Baou de Saint-Marcel oppidum, in segobrige territories
46 east of Massalia, is made of a vuggy limestone whose clotted peloidal-fenestral fabric and
47 isotope signature are consistent with local, lower Pleistocene travertines. The *young male head*
48 from the Ziem Museum revealed to be made of a planktonic foraminiferal, quartz-free limestone
49 with *Heterohelix* for which no analogue is known in the region, thus suggesting that its place
50 of manufacture is likely to be located outside Provence. Finally, the analyzed set of limestones
51 from protohistoric sculptures, and of certain Provençal provenance, derive from stone
52 production sites geographically close (<20 km) from the places of discovery. A set of non-
53 invasive in situ techniques has been also used to discriminate among the possible sources
54 (magnetic susceptibility, X-ray fluorescence chemical analysis, sound velocity,
55 photogrammetry), but they appeared non discriminant for the present case.

56

57 **Key-words:** sculptural limestones, provenance, protohistory, petrography, stable isotopes, non-
58 destructive methods, Provence, Gaul.

60 **1.Introduction**

61

62 In the last decades, following major discoveries of statues in Germany and France in particular
63 (e.g. Frey and Hermann, 1997; Menez et al., 1999), European protohistoric sculpture has re-
64 emerged as a topic of interest in archaeology and art history. Provence represents one of the
65 most prolific regions for its corpus of protohistoric sculptures (Duceppe-Lamarre, 2002;
66 Arcelin and Rapin, 2003). Stylistic analyses and detailed characterization of the archaeological
67 setting of these statues constitute major inputs for positioning protohistoric Provence within a
68 European cultural framework. In this context, provenance analyses allow to discriminate a local
69 or regional origin for the statuary material and to identify potential importations. Such studies
70 are particularly useful when the place of discovery of statues is uncertain or their archaeological
71 setting poorly constrained. Additionally, such provenance studies provide significant insights
72 into stone artefact production and trading in ancient times. Following the terminology used by
73 Flügel and Flügel (1997), local material is defined as material extracted at the site where statues
74 were discovered, regional material derives from outcrops located within a distance of several
75 tens of kilometers while the term 'imported' should refer to lithic material brought from far
76 distances. Microfacies analysis combined with micropaleontological and/or geochemical
77 approaches on chips detached from artefacts have revealed to provide a means of distinguishing
78 between local, regional and imported materials (e.g. Attanasio et al., 2000; Capedri et al., 2001;
79 Sanmarco et al., 2015; Brilli et al., 2011). Moreover, non-invasive in situ techniques are more
80 and more demanded to avoid sampling patrimonial cultural objects. They proved for example
81 to be effective for the study of rocks such as obsidian, granite, sandstones and greywacke
82 (Frahm et al., 2013; Williams-Thorpe et al., 2009; Rochette et al. 2022; Ushida et al, 2021).
83 The present work focuses on the provenance of statuary limestones of a set of six protohistoric

84 statues from various localities in Provence and hosted at the Musée d'Histoire de Marseille
85 (MHM) (**Fig. 1 A-F**). Additionally, a male head sculpture (**Fig. 1G**) hosted in the Ziem Museum
86 of Martigues and whose site of discovery is unknown, has been integrated in the present work.
87 The objective of the provenance study performed on this set of protohistoric statues is mainly
88 to answer the following questions: 1) did the sculptor used local, regional or imported
89 limestone? 2) can the statuary limestone material be traced to specific areas and production
90 sites? 3) do production sites of sculptural limestones coincide with those of building stones?

91

92 **2.Archaeological and geological setting of protohistoric sculptures**

93

94 **2.1 Roquepertuse oppidum**

95 The Roquepertuse oppidum (**Fig. 2A**) is a protohistoric site located in the municipality of
96 Velaux which yielded one of the most important statuary group from Provence (Gérin-Ricard,
97 1927; Boissinot, 2011, Py 2011). The set of sculptures analyzed in the present work, a *warrior*
98 *seated cross-legged* (**Fig. 1A**), a *lintel with horses* (**Fig. 1B**) and the *twin-headed "Hermes"*
99 (**Fig. 1C**), were discovered on a terrace located in the southern flank of the oppidum, and they
100 were first interpreted as elements of a sculptural monument known as a "portique" dated to the
101 3rd-2nd century BC. The age of the statues remains very controversial. Although the stratigraphic
102 position of most of the statues discovered during early excavations is poorly constrained, a
103 revision of the chronology of the site was undertaken, following excavations carried out
104 between 1994 and 1999, leading to assign the habitat to the first half of the 3rd century BC while
105 the lapidary material (lintels, seated warriors), found as fragments scattered within the whole
106 settlement had to be considered older (Boissinot et al., 2000). Stylistic studies have contradicted
107 this attribution and have suggested an age from the transition between the First and Second Iron

108 Ages to the beginning of the Second Iron Ages, i.e. from 525 to 375 BC (Arcelin and Rapin,
109 2003; Rapin, 2004).

110 The Roquepertuse oppidum rests on the flanks and on top of a flat-topped hill composed of
111 nodular and marmorized continental limestones, latest Campanian to earliest Maastrichtian
112 (“Calcaire de Rognac” formation) in age (**Fig. 3A**).

113

114 **2.2 Rognac**

115 The *warrior seated cross-legged* from Rognac (**Fig. 1D**) was discovered at the beginning of the
116 20th century in a dry stone wall at a place called "Plan du Clapier" (Clerc, 1914; Py (2011),
117 located north of the town of Rognac (**Fig. 2A** and **Fig. 3B**). This statue having been reused as
118 a building material, its initial place of use is unknown but it may derive from a neighboring
119 oppidum, such as Le Castellans oppidum located 3 km to the south-east, or Roquepertuse (5 km
120 to the north-east). The stylistic analysis of the statue has led to compare the Rognac statue with
121 the seated warriors from Roquepertuse and then to assign them an age ranging from 525 to 375
122 BC (Arcelin and Rapin, 2003).

123 The place of discovery is located on a plain covered with late Pleistocene colluvium, while the
124 neighbouring Le Castellans oppidum rests on uppermost Campanian to lowermost Maastrichtian
125 continental limestones (“*Calcaire de Rognac*” formation) (**Fig. 3B**).

126

127 **2.3 La Cloche oppidum**

128 A set of fragments belonging to the same statue was discovered at La Cloche oppidum, at Les
129 Pennes-Mirabeau (**Fig. 2A** and **Fig. 3C**) in 1975, which allowed reconstructing a bust of warrior
130 (**Fig. 1E**). La Cloche oppidum is a settlement of the first half of the 1st century BC, while a prior
131 ritual deposit dated of the end of the 3rd-2nd century BC (Chabot, 1996, 2005) was discovered
132 at the top of the site. The fragments were found on a street at the entrance area of the 1st century

133 BC settlement, but could come from the cultural area. Its fragmentation is believed to be related
134 to the final destruction of the oppidum by Caesar's troops in -49 (Chabot, 1983, 2004).
135 Regarding stylistic studies, while Chabot (2005) attributes to the head a massaliote influence,
136 Arcelin and Rapin (2003) suggest a much older age, i.e from the end of the 4th century to the
137 middle of the 3rd century BC. The oppidum rests on tight and fractured Barremian limestones
138 with rudists (Urgonian facies) (**Fig. 3C**).

139

140 **2.4 Baou de Saint-Marcel oppidum**

141 The Baou de Saint-Marcel oppidum is a fortified Celto-Ligurian, Segobrige settlement site,
142 located in the eastern districts of Marseille (**Fig. 2A** and **Fig. 3D**), founded at the end of the first
143 quarter of the 6th century BC and abandoned in the last quarter of the 2nd century BC (Agostini,
144 1972; Guichard and Rayssiguier, 1993). It rests on the top of a flat-topped hill made of
145 Pleistocene calcareous tufa (**Fig. 3D**). The studied material from Baou de Saint-Marcel
146 oppidum is an element of the edge of the dorsal part of a rectangular and rigid scapular tunic
147 (**Fig. 1F**) belonging to a limestone statue. This fragment has been found in a reworked context,
148 interpreted as metal deposit, located under the collapse of the southern bastion of the eastern
149 rampart (Rayssiguier, 1989 ; Rayssiguier and Guichard, 1989 ; D'Ovidio and Rothé, 2005 ;
150 Dedet and Gantès, 2014), containing also metal furniture, ceramic and a silver obolus from
151 Marseille which, in spite of the dominance of artefacts from the 6th century BC, give a broad
152 dating ranging from the 6th to the 2nd century BC. However, according to Py (2011), the
153 scapular tunic from Baou de Saint-Marcel closely resembles that of the seated warriors of
154 Roquepertuse and could be of a neighboring age, i.e. 3rd century BC.

155

156 **2.5 Ziem Museum**

157 The Ziem Museum in Martigues acquired from a local collector a limestone juvenile male head
158 evaluated as being a work of high empire style and probably sculpted in a workshop from the
159 south of Gaul (D. Terrier, CCJ, Ziem Museum internal document) (**Fig. 1G**) but without any
160 documentation regarding the site of discovery. Despite its great interest it is not exposed due to
161 the uncertainty of its provenance.

162

163 **3. Database and methods**

164

165 **3.1 Sampling**

166 For laboratory characterization of the statuary material (thin-section preparation and
167 stable isotope measurements), we were allowed by the museums to detach a small chip (at most
168 one gram) from areas without significant sculpted surface, i.e. previous fractures limiting
169 excavated fragments. We obtained three samples from different objects of the Roquepertuse
170 provenance (see above), and one sample per statue from the other four provenances. A number
171 of potential source local and regional material have been sampled on geological outcrops to be
172 compared with statuary material (see **Table 1**). We also based our methodology on our database
173 derived from numerous petrological and petrophysical studies of regional limestones.

174

175

176 **3.2 Thin-section database and petrographic analysis**

177 The petrographic study of the seven limestone sculptures has been performed by means of
178 macroscopic direct observations of lapidary collections at the MHM (Musée d'Histoire de
179 Marseille) and at the Ziem Museum and analysis of thin-sections under polarized-light

180 microscopy. Thin-sections were prepared from the seven chips extracted from the sculptures.
181 An existing thin-section database of regional limestones from outcrops (**Table 1**), hosted at
182 CEREGE laboratory (Marseille), has been integrated in this study for qualitative and
183 quantitative comparison with the statuary material. Thin-sections were also prepared from local
184 limestones sampled at or at the vicinity of the oppida. Additional thin-sections of ancient
185 building stones from the Hellenistic harbor of Massalia, housed at the CICRP have been also
186 integrated. Thin-sections have been studied for microfacies characterization of limestone
187 including texture, grain composition, biotic assemblages and diagenetic features. Additionally,
188 a selection of thin-sections of both sculptures and outcrops were point-counted on the basis of
189 300 points to quantify the composition of the sand-grained fraction of limestones by using J-
190 microvision® software.

191

192 **3.3 Scanning Electron Microscopy (SEM)**

193 In order to identify the microstructure of limestone at a micrometer-scale and to check the
194 elemental composition of minerals, small fragments (~5 mm in diameter) from the statuary
195 limestones were imaged with the Philips XL 30 Environmental Scanning Electron Microscope
196 (ESEM) of the Plateforme de Recherche Analytique Technologique et Imagerie (PRATIM,
197 Aix-Marseille University, FSCM, France), equipped with a LaB6 filament and Energy
198 Dispersive X-Ray analysis (EDAX Genesis equipped with an Apollo 10 SDD detector). The
199 analytical settings used were: 20 keV; back-scattered electron mode BSE; no carbon-coating;
200 pressure of 0.2 Torr.

201

202 **3.4 Stable isotopes**

203 Carbon and oxygen stable isotope ratios ($\delta^{13}\text{C}$ and $\delta^{18}\text{O}$) have been measured on bulk
204 carbonate powders from statuary limestones, local limestones from Roquepertuse, Le Castellas

205 (Rognac), La Cloche and Baou de Saint-Marcel oppida and selected limestones from regional
206 outcrops and from building stones belonging to the hellenistic Massalia harbour. The carbon
207 and oxygen stable isotope database used for this study is summarized in **Table 2** while the
208 measurements are displayed in the **Appendix**.

209

210 Measurements on statuary and local limestones as well as on regional limestones from Coudoux
211 have been performed using a Dual-Inlet Isotope Ratio Mass Spectrometer (DI-IRMS Delta V
212 Plus, Thermo Scientific) coupled to an automated carbonate preparation line (Carbonates
213 Device Kiel IV, Thermo Scientific) at CEREGE platform for stable isotope analysis (PANISS).
214 Carbonate powders from Upper Barremian (« Pierre de Cassis »), Upper Burdigalian-Langhian
215 (« Pierre de La Couronne ») limestones and Pleistocene calcareous tufa were carried out at the
216 GeoZentrum Nordbayern department, Friedrich-Alexander-Universität Erlangen-Nürnberg
217 (Germany) through reaction with phosphoric acid at 70°C using a Gasbench II connected to a
218 Thermo Fisher Scientific DELTA V Plus mass spectrometer.

219 All measured isotopic values are normalized against NBS-19 and are expressed relative to the
220 V-PDB standard. Mean external reproducibility is better than 0.05‰ and 0.07‰ for $\delta^{13}\text{C}$ and
221 $\delta^{18}\text{O}$ respectively.

222

223 **3.5 Non-invasive techniques**

224 We tested several techniques that were applicable directly on the statues in the museum without
225 surface preparation:

226 1) Magnetic susceptibility (K) measurements were performed on statues using the SM30
227 sensor whose detection volume is a 5 cm diameter cylinder below the coil. Sensitivity

228 is a few 10^{-6} SI, depending on the presence of surrounding metal. Contribution to the
229 signal decreases with depth and 69% of it derives from the first cm. Corrections are
230 needed to account for surface unevenness and curvature as the sensor is calibrated for a
231 perfectly flat surface (Rochette et al., 2022). For geological samples, the most sensitive
232 instrument MFK1 Kappabridge, was used.

233 2) Chemical analysis using portable X-ray fluorescence instrument. We have used the
234 Bruker tracer IV, in major trace element mode with a counting time of 90 s for each
235 mode. It has an analysis spot size of the order of 1 cm and a penetration depth in the 10-
236 1000 μm depth range depending on the elements analysed and thus the energy of re-
237 emitted X-rays. It shows a sensitivity on trace elements such as Rb and Sr contents of
238 the order of 5 ppm while light major elements have a much higher detection limit: e.g.
239 near 2 and 4-5% for Al and Mg, respectively. We used several measurement spots per
240 statue or sample (usually 5) and calculate the average results. The methodology for such
241 measurements has been recently detailed in Triantafyllou et al. (2021).

242 3) Velocity of sound (V_p). In limestones V_p determination is a good proxy for porosity
243 and pore structure, that may be used to discriminate among different formations and
244 outcrops. We used a PUNDIT PL 200, with a peak frequency of 54 kHz.

245 4) Bulk density and porosity estimate. Bulk density ρ_b was obtained by weighting the
246 statues or the geological samples cut as parallelepipeds, and determining their volume
247 using photogrammetry and edge dimensions, respectively. As we deal with nearly pure
248 limestones, porosity estimate (Φ) was computed by the formula $\Phi = (1 - \rho_b/\rho_c) \times 100$,
249 where ρ_c is the density of pure calcite, i.e. $2.71 \cdot 10^3 \text{ kg/m}^3$.

250

251

252 **3.6 Photogrammetry**

253 The *Twin-headed "Hermes"*, the *Bust of Warrior* from La Cloche and the *Young Male Head*
254 from the Ziem Museum have been scanned in 3D by close-range photogrammetry (**Fig 1H**).
255 For acquisition, we have set up each statue in several positions on a table, and we have captured
256 around 100 pictures per position at different angles in a convergent way. The camera used is a
257 high-grade DSLR Sony Alpha 7 R4 with a FE 50mm F1.2 Zeiss lens. The sensor is full-frame,
258 9504x6336 pixels BSI-CMOS with 63 megapixels. Pictures were processed with Capture One
259 v20 software. We made a color calibration with the ColorChecker® Classic chart from X-Rite
260 and its software ColorChecker Camera Calibration v2.2.0, allowing to create a custom ICC
261 color profile for each lighting condition. Photogrammetric processing was undergone with
262 Agisoft® Metashape v1.8 software using a standard workflow (Brunier et al., 2016). All photos
263 were aligned in separate chunks for each statue position. We obtained a very high-resolution
264 point cloud, with density 5 pts/mm², and low accuracy value with RMSE lower than 1 mm for
265 each processing. Triangular meshes have been interpolated from point cloud, and texture of
266 photos were projected on them. The meshes have been used to derive volume and area of the
267 statue.

268

269 **3.7 Provenance assessment methodology**

270 We will show that the used non-destructive techniques revealed to be not effective to
271 discriminate among the different limestones investigated. Therefore, provenance assessment of
272 statuary limestones studied here will be based on the following workflow:

273 1- Detailed petrography (depositional facies and diagenetic features) of statuary limestones,
274 stable isotope (C and O) signatures and stratigraphic attribution using available microfossils;

275 2- Consistency between facies, diagenetic features, isotope signatures and age of statuary
276 limestones and local limestone. If consistent, a local origin is privileged otherwise a regional
277 origin must be investigated.

278 3- Identification, from published literature, of regional formations sharing the following
279 properties: 1) similar geological age to that of the statuary material, 2) similar depositional
280 facies and environments, 3) mechanical properties compatible with use for sculpture.

281 4- Creation of a database of thin-sections and stable isotope signatures for these identified
282 formations from existing or newly acquired field data and laboratory measurements.

283 5- From the available database, identification of intervals and localities where depositional
284 facies (characterized quantitatively), diagenetic features and stable isotope signatures are
285 analogous to those of statuary limestones. Such intervals and localities will be considered as
286 probable areas of provenance of the statuary material.

287 6- Comparison of such potential localities with ancient sites of stone production and critical
288 evaluation of provenance assessment within the archaeological context.

289

290 **4. Results**

291

292 **4.1 Petrographic analysis of statuary limestones**

293

294 **4.1.1 Roquepertuse oppidum**

295

296 4.1.1.1 The *twin-headed "Hermes"*

297 Macroscopically, the *twin-headed "Hermes"* from Roquepertuse is made of a homogeneous
298 fine-to-medium grained limestone with a slightly reddish patina, and chalky aspect on fresh
299 sections. Observations under optical microscopy reveal that the *twin-headed "Hermes"* (**Fig.**

300 **4A)** is composed of a well-sorted grainstone, largely dominated by ooids (78%), with minor
301 proportion of bioclasts (12%) and peloids (9%). The biota includes benthic foraminifers
302 (miliolids and orbitolinids), echinoids and sparitized fragments of molluscs and green algae.
303 Grain size averages 300 μm . The ooid cortices were partly leached and ooid nuclei appear
304 commonly suspended in the middle of moldic cavities created by leaching (**Fig. 4B-C**). Such
305 dissolution molds are partially filled with sparse equigranular sparry calcite crystals (20-50 μm)
306 (**Fig. 4D-E**). Ooids are surrounded by a thin ($\sim 20 \mu\text{m}$) isopacheous rim of palisade calcite
307 cement (**Fig. 4D-E**) while the intergranular space is completely occluded by coarser ($>50 \mu\text{m}$)
308 blocky calcite cement. Most of the grains are strongly micritized and exhibit significant
309 microporosity between micrite particles under SEM microscopy (**Fig. 4D**). The outer surface
310 of peloids commonly shows evidences of dissolution having led to the development of a
311 perigranular porosity.

312

313 4.1.1.2 The Warrior seated cross-legged

314 Macroscopically, the *warrior seated cross-legged* from Roquepertuse is made of a
315 homogeneous fine-to-medium grained limestone with a light beige patina, slightly chalky on
316 fresh sections. Observations under optical microscopy reveal that the statuary material is made
317 of a well-sorted grainstone (**Fig. 5A**) mainly composed of bioclasts (44%), ooids (29%) and
318 peloids (27%). Grain size averages 200 μm . The bioclastic association is similar to that of the
319 *twin-headed "Hermes"* limestone and is dominated by benthic foraminifers such as miliolids
320 and orbitolinids, together with echinoids, pieces of molluscs and green algae. In both samples,
321 the outer parts of ooids and micritized grains are significantly leached and similarly to the *twin-*
322 *headed "Hermes"* grainstone, the resulting perigranular moldic cavities are partially occupied
323 by sparse equigranular sparry calcite crustals (**Fig. 5B-C**). Most of the grains (benthic

324 foraminifers, ooids and peloids) are strongly micritized and exhibit, under SEM observation a
325 significant microporosity between micrite particles.

326

327 4.1.1.3 The lintel with horses

328 The *lintel with horses* is made of a homogeneous, medium to coarse-grained limestone
329 with light beige patina. The microfacies consists in a well-sorted bioclastic grainstone (**Fig. 5D**)
330 dominated by bioclasts (75%) including rounded and sparitized fragments of rudists and coral,
331 benthic foraminifers (miliolids and orbitolinids) and peloids (25%). The outer part of most of
332 the grains is significantly micritized (micrite envelope) and/or leached (**Fig. 5D-E**). The
333 intergranular space is partly occluded by an isopachous rim of bladed calcite cement postdated
334 by coarser equigranular calcite cement (**Fig. 5E**). Intergranular porosity may be partly preserved
335 in large pores (**Fig. 5E**). The microfacies differs from that of the *twin-headed "Hermes"* and to
336 the *warrior seated cross-legged* from Roquepertuse in being slightly coarser (average grain
337 size: 500 μm) and devoid of ooids.

338

339 **4.1.2 Rognac**

340

341 The *warrior seated cross-legged* from Rognac is made of a medium to coarse-grained,
342 homogeneous, light beige limestone. Similarly to Roquepertuse statuary limestones, fresh
343 sections exhibit a slightly chalky texture. Observations under optical microscopy (**Fig. 5F**)
344 show that the Rognac limestone is a bioclastic grainstone (average grain-size: 500 μm) with
345 very similar composition to that of the *Lintel with horses* from Roquepertuse. Bioclasts (71 %),
346 including miliolids, orbitolinids, mollusk fragments and echinoderms dominate the grain
347 association, while peloids (29%) are subordinate components. Additionally, diagenetic features
348 are identical to those evidenced in Roquepertuse statuary limestones: significant perigranular

349 porosity around grains (**Fig. 5G**), partial infills of molds by equigranular calcite and blocky
350 calcite cements.

351

352 **4.1.3 La Cloche oppidum**

353

354 The *bust of warrior* from La Cloche oppidum is macroscopically made up of a fairly
355 heterogeneous, vuggy, bioclastic limestone exhibiting a pinkish patina. Thin section
356 observations under polarized-light microscopy point towards a bioclastic packstone-grainstone
357 (**Fig. 6A-B**) whose biological assemblage is largely dominated by bryozoans (46%) and
358 echinoderms (39%), the subordinate biota being mainly composed of benthic foraminifers
359 (*Amphistegina*), coralline algae and mollusks. The matrix is composed of very fine peloids
360 (<100 μm) and occupies partially the intergranular space. The residual intergranular space is
361 partially filled by equigranular sparry calcite cement. Poikilotopic cements may occlude some
362 large intergranular pores.

363

364 **4.1.4 Baou de Saint-Marcel oppidum**

365 Macroscopically, the fragment of scapulary from Baou de Saint-Marcel oppidum is made of a
366 limestone with a slightly yellowish patina, exhibiting abundant microvugs (<1 mm).
367 Observations under optical microscope (**Fig. 6C-D**) show that the sample consists of an
368 assemblage of peloids of irregular shape connected to each other by micritic bridges (= clotted
369 peloids) encasing fenestral pores (typically 100-500 μm in diameter). In addition to this
370 dominant microfabric, peloidal encrustations around plant stems are also present (**Fig. 6D**), the
371 stems being preserved as voids. The clotted peloidal fabric, the dominant fenestral porosity as
372 well as encrustations around plants allow identifying a calcareous tufa.

373

374 **4.1.5 Ziem Museum statue**

375 The *Young male head* statue from the Ziem Museum is made of very homogeneous, very tight
376 limestone with a dark beige patina. Under polarized-light microscopy, this limestone is a very-
377 fine grained grainstone-packstone composed dominantly of fragments of planktonic
378 foraminifera (**Fig. 6E**) including biserial (*Heterohelix*: **Fig. 6F**) and planispiral (cf.
379 *Hedbergella*) taxa. Observations under SEM reveal that the matrix is partly to entirely
380 composed of fragments of coccoliths (**Fig. 6G**).

381

382 **4.2 Petrographic analysis of local limestones**

383

384 **4.2.1 Roquepertuse oppidum**

385 The continental upper Cretaceous deposits outcropping at the Roquepertuse oppidum are
386 dominantly composed of nodular, marmorized limestones. The microfacies consists of a
387 pisolithic packstone with numerous cracks and root traces (**Fig. 7A**) indicative of pedogenic
388 limestones.

389

390 **4.2.2 Le Castellans oppidum**

391 The continental upper Cretaceous (Maastrichtian) deposits outcropping at Le Castellans
392 (Rognac) oppidum are dominantly composed of tight, fractured and karstified limestones. The
393 microfacies consists of bioclastic wackestones with characean gyrogonites and stems (**Fig. 7B**)
394 as well as common gastropods. Early pedogenic features are common (root traces and
395 circumgranular cracks) thus suggesting a deposition in palustrine environments.

396

397 **4.2.3 La Cloche oppidum**

398 Barremian limestones outcropping at La Cloche oppidum are dominantly tightly cemented
399 bioclastic and peloidal packstone to grainstones (**Fig. 7C**). The biota is dominated by rudist
400 fragments and benthic foraminifera including miliolids and orbitolinids.

401

402 **4.2.4 Baou de Saint-Marcel oppidum**

403 Pleistocene calcareous tufa from Baou de Saint-Marcel oppidum are characterized by clotted-
404 peloidal fabrics as well as by micritic and sparitic encrustations around phytoliths or peloids
405 (**Fig. 7D**). Larger (>1 mm) oncoids are also common.

406

407 **4.3 Stable isotopes**

408 Stable isotope results ($\delta^{13}\text{C}$ and $\delta^{18}\text{O}$) on bulk carbonate powders from the selected statuary
409 limestones are displayed in **Fig. 8A**. Roquepertuse and Rognac statues display very close values
410 of $\delta^{13}\text{C}$ (-0.71 to -0.07 ‰) and $\delta^{18}\text{O}$ (-5.93 to -5.05 ‰). Measurements on the *Bust of Warrior*
411 from La Cloche are significantly ^{13}C and ^{18}O -depleted compared to Roquepertuse and Rognac
412 statues with $\delta^{13}\text{C}$ and $\delta^{18}\text{O}$ averaging -2.51‰ and -6.28 ‰ respectively. The fragment of
413 scapulary from Baou de Saint-Marcel exhibits both highly negative $\delta^{13}\text{C}$ and $\delta^{18}\text{O}$ values (-5.97
414 and -6.40 ‰ respectively) which are consistent with continental carbonates (Deocampo, 2009).
415 Results from the Ziem Museum statue stands out from other measurements by positive $\delta^{13}\text{C}$
416 values (averaging +0.78 ‰) and slightly ^{18}O -enriched composition with $\delta^{18}\text{O}$ averaging -4.29
417 ‰. The comparison between statuary and local limestone isotope composition (**Fig. 8A**)
418 suggests a non-local origin for the statues of Roquepertuse, Rognac and La Cloche. In contrast,
419 the very ^{13}C and ^{18}O -depleted values of the calcareous tufa from Baou de Saint-Marcel outcrops
420 are consistent with those of the scapulary fragment.

421 Additionally, an isotopic database ($\delta^{13}\text{C}$ and $\delta^{18}\text{O}$) of limestones from Provence, likely to
422 provide statutory material, has been achieved in order to make the attributions of provenance of
423 the different statues more robust. Such a database integrates original measurements (**Table 2**
424 and **Appendix**) as well as published data (Léonide *et al.*, 2014; Aubert *et al.*, 2020). The Upper
425 Barremian “*Pierre de Cassis*” (“*Cassis Stone*”), a tight limestone which is very widely used in
426 the region as a building stone or in sculpture (Tréziny, 2009) is characterized by positive $\delta^{13}\text{C}$
427 values ranging from +0.17 to +3.01‰ (**Fig. 8B**). In contrast, chalky Upper Barremian
428 limestones from Martigues are significantly ^{13}C and ^{18}O -depleted compared to time-equivalent
429 facies from Cassis. The Lower Barremian “*Pierre de Calissane*” is a chalky limestone which
430 was extensively quarried in La Fare Massif area and which is characterized by dominantly
431 negative $\delta^{13}\text{C}$ values and by a rough positive covariant trend between $\delta^{13}\text{C}$ and $\delta^{18}\text{O}$ (**Fig. 8B**).
432 Samples from an abandoned quarry located in Coudoux show slightly negative $\delta^{13}\text{C}$ values
433 (from -1.04 to -0.70‰) while $\delta^{18}\text{O}$ range from -5.23 to -5.11‰. The Upper Burdigalian-
434 Langhian “*Pierre de La Couronne*” is a regionally famous building stone used since Antiquity
435 which makes up most of the hellenistic buildings from the Massalia harbour (Pédini, 2013). On
436 $\delta^{13}\text{C}$ - $\delta^{18}\text{O}$ cross-plot (**Fig. 8B**), “*Pierre de La Couronne*” measurements cover a wide domain
437 with dominantly negative $\delta^{13}\text{C}$ values (-5.30 to 0.29‰) and $\delta^{18}\text{O}$ ranging from -6.93 to -1.02‰.
438 Although $\delta^{13}\text{C}$ - $\delta^{18}\text{O}$ domain of Upper Burdigalian-Langhian limestones partially overlaps that
439 of Barremian limestones, isotope composition of “*Pierre de La Couronne*” samples are
440 typically more ^{13}C -depleted for a given $\delta^{18}\text{O}$ value. Additionally, the present “*Pierre de La*
441 *Couronne*” isotope database reveals a decreasing trend in $\delta^{18}\text{O}$ from east (Tamaris section) to
442 west (Anse du Verdon section). Isotope signatures of building stones from the hellenistic
443 Massalia harbor are consistent with the western area (Anse du Verdon) isotope composition.
444 Finally, the isotope signature of Pleistocene calcareous tufa stand out very clearly by their very
445 negative $\delta^{13}\text{C}$ values (-9.61 to -4.53‰).

446

447 **4.4 Non-destructive analyses**

448 In the course of our study, it appeared that the studied material presents a number of
449 unfavorable characteristics to obtain reliable results with the deployed techniques. Statues are
450 fragmentary and have been reassembled using cement and steel bars. They also show numerous
451 holes and fractures. Such characteristics will obviously bias the sound velocity measurements
452 as well as magnetic measurements. Magnetic susceptibility measurements on the statues were
453 hardly measurable: K always below $2 \cdot 10^{-5}$ SI, apart from spots affected by the steel bars. This
454 is close to noise level in the museum conditions and typical of un-metamorphosed platform
455 carbonates, with negligible magnetite and limited clay contents, and does not allow any
456 discrimination. On geological samples, K was negative, i.e. diamagnetic. Sound velocity
457 measurements on the statues show strong variability, from 2 to 4.5 km/s (**Table 3**) and cannot
458 obviously be used for lithological determinations.

459 Porosity estimates (**Table 3**) vary from 5 to 25%. The value measured for the *twin-headed*
460 “*Hermes*” from Roquepertuse (17.4 %) is in the high range observed for Coudoux outcrop
461 samples, likely possibly due to the alteration of the statues. The three pieces of the la Cloche
462 statue yield coherent porosities, with an average of $20.4 \pm 2.1\%$, identical to the value measured
463 in La Couronne limestone at Baou Tailla quarry (west of Anse du Verdon). The Ziem head has
464 the lowest porosities of the studied statues (12.6 %) in agreement fine the petrographic
465 observations.

466 Chemical analysis by pXRF may be contaminated by products pasted on the statue surfaces
467 after their fabrication. This may be intentional (painting from the in-use period or unfortunately
468 applied by early 20th century archeologists; artificial patina applied in the museum to
469 homogenize color or fill holes) or incidental: contamination by soil within which the material

470 was buried, or by dust accumulated in the surface porosity since discovery. pXRF results (**Table**
471 **3**) are obviously affected by the state of the statue surface: determined CaO content varies from
472 37 to 62 wt.%, while is always higher than 82 % (and mostly in the 91-95% range) for
473 geological equivalent samples, measured on sawn surfaces. To compensate this effect we
474 normalized other elements to CaO. MgO/CaO ratios are in the range 90 to 240 ‰, on the statues
475 as well as on geological samples. These high values are in contradiction with the petrographic
476 observations that do not show the presence of dolomite. However, Mg quantification is
477 problematic with the pXRF instrument. Al₂O₃/CaO, SiO₂/CaO, ratios are systematically higher
478 on statues (up to 70 and 180 ‰, respectively) than on geological samples (around 20 ‰ for
479 both ratio). The same is true for Fe/Ca and K/Ca. This clearly signs a contamination, either by
480 soil or cement applied in the museum. In all geological samples (except Baou-Tailla) Fe/Ca is
481 below 4 ‰ confirming diamagnetic magnetic susceptibility. Significant contents of Ti, Zn, Pb
482 are sometimes observed only on the statues (not reported in Table 3), again pointing toward a
483 contamination (modern painting, urban pollution?).

484

485 **5. Discussion**

486 **5.1 Provenance assessment of protohistoric statuary limestones from Provence**

487

488 ***5.1.1 Roquepertuse and Rognac statues***

489 The studied statuary material from Roquepertuse and Rognac exhibits common
490 sedimentological, diagenetic and geochemical characteristics: 1) chalky character of the
491 limestone linked to significant microporosity, 2) depositional texture (grainstone) and faunal
492 association composed predominantly by miliolids, orbitolinids and rolled fragments of rudists,
493 3) the presence of perigranular dissolution features around micritized grains and 4) a very

494 homogeneous carbon and oxygen isotope signature with values ranging from -5.0 to -5.9‰ in
495 $\delta^{18}\text{O}$ and from -0.1 to -0.7 ‰ in $\delta^{13}\text{C}$.

496 Members of the larger benthic foraminiferal family Orbitolinidae occurred from the early
497 Cretaceous to the Oligocene (Boudagher-Fadel and Price, 2019) and in Provence, they are
498 reported from the Berriasian (Virgone, 1997) to the Coniacian (Babinot and Tronchetti, 1983).
499 The observed microfacies (**Fig. 4** and **5**) suggest outer carbonate platform environments
500 (Leonide et al., 2012). Both age and depositional environments contradict a local origin of the
501 statuary material, the oppida of Roquepertuse and Le Castellas (Rognac) being located on upper
502 Cretaceous continental limestones. Regionally, chalky, microporous grainstones from the inner
503 to outer Barremian carbonate platform have been reported in Martigues area, La Fare Massif as
504 well as in Mont-de-Vaucluse (Borgomano *et al.*, 2013; Léonide *et al.*, 2014). As a consequence,
505 based on 1) the Cretaceous age inferred from faunal associations, 2) the shallow carbonate
506 platform environments suggested by microfacies and 3) the chalky, microporous nature of the
507 statuary material, a regional Barremian origin is hypothesized for the limestone composing both
508 Roquepertuse and Rognac statues.

509 To validate such a hypothesis, a regional thin-section and stable isotope database (**Table 1** and
510 **3**) has been integrated and an additional field section has been surveyed at Coudoux (**Fig. 1** and
511 **Fig. 9**), which represents the closest locality to the studied oppida with Barremian outcrops (3.6
512 km from Roquepertuse and 7 km from Rognac). At Coudoux the upper 50 meters of the lower
513 Barremian chalky limestones crop out in the southern flank of the La Fare Massif, where they
514 are sharply truncated at top and overlain by late Cretaceous deposits (**Fig. 9B**). This carbonate
515 succession consists of an alternation of four depositional facies (**Fig. 9A**): 1) oolitic grainstones
516 (Facies BF1: ooid proportion >50%), 2) oobioclastic grainstones (Facies BF2: ooid
517 proportion <50%), 3) bioclastic grainstones (Facies BF3: no ooid and bioclast content >50%),
518 and 4) bioclastic rudstones (Facies BF4). Examinations of thin sections revealed that the facies

519 association of Coudoux is analogous with that of the statuary limestones from Roquepertuse
520 and Rognac regarding depositional texture, grain-size, allochemical composition and diagenetic
521 features (**Fig. 10**). The COU-A sample from Coudoux is a fine-to-medium grained oolitic
522 grainstone where ooids represent 59% of the grains while subordinate components are bioclasts
523 (31%) and peloids (10%), the bioclastic assemblage being composed of rolled sparitized rudists,
524 benthic foraminifers (mainly miliolids and orbitolinids) and echinoderms (**Fig. 10A**).
525 Additionally, the cortex of ooids exhibit similar dissolution features (**Fig. 10D**) as those
526 evidenced in Roquepertuse statues (**Fig. 4B-C** and **5B-C**). As a consequence, the COU-A
527 sample is quantitatively and qualitatively extremely close from the fine-to-medium grained
528 oolitic grainstone of the Twin-headed “Hermes” from Roquepertuse (ooids: 66%; bioclasts:
529 21%; peloids: 13%). Similarly, the sample COU-B (oobioclastic grainstone: facies BF2) is an
530 analogue (**Fig. 10B**), regarding texture, grain-size (fine-to-medium), diagenetic features
531 (leached cortex of ooids) and grain composition (ooids: 41%; peloids: 26%; bioclasts: 33%) of
532 the statue of warrior from Roquepertuse (ooids: 41%; peloids: 26%; bioclasts: 33%). Finally,
533 the *lintel with horses* from Roquepertuse (peloids: 28%; bioclasts: 72%) and the *warrior seated*
534 *cross-legged* from Rognac (peloids: 36%; bioclasts: 64%) are bioclastic grainstones (Facies
535 BF3) of similar composition with the COU-C sample from Coudoux (peloids: 32%; bioclasts:
536 68%) (**Fig. 10C**). These results are therefore consistent with a common provenance, within the
537 lower Barremian chalky limestones of La Fare Massif, for the studied statues from
538 Roquepertuse and Rognac. Such a provenance is also supported by carbon and oxygen isotope
539 signatures of the statuary limestones which fall within the $\delta^{13}\text{C}$ - $\delta^{18}\text{O}$ domain of chalky lower
540 Barremian limestones from La Fare Massif and which are extremely close from values
541 measured in Coudoux samples (**Fig. 11A**). West of Coudoux, the lower Barremian chalky
542 limestones passes laterally into dominantly bioclastic grainstone facies and ooids are almost
543 lacking as evidenced in ancient quarries at Calissanne (Borgomano et al., 2013). As a

544 consequence, even if a common provenance, at Coudoux, for the 4 sculptures from
545 Roquepertuse and Rognac is very probable, it is not excluded that the *Lintel with horses* from
546 Roquepertuse and the *warrior seated cross-legged* from Rognac, both made of bioclastic
547 grainstone (BF3), come from a more western sector of the La Fare Massif (distant up to 15 km
548 from Roquepertuse). The petrographic and geochemical analyses of the three statues of
549 Roquepertuse confirm the intuition of Gérin-Ricard (1927) according to which the material of
550 the sculptures of Roquepertuse should derive from neighbouring outcrops at Coudoux. More
551 recently, Lescure and Werth (2000) compared the X-ray diffraction spectra of Roquepertuse
552 and Coudoux samples and have shown that both limestones are almost purely calcitic.

553 We note that porosity estimates are coherent between the Coudoux geological samples
554 and the Roquepertuse and Rognac statues.

555

556 **5.1.2 The bust of warrior from La Cloche**

557 The occurrence of the benthic foraminifera *Amphistegina* in the *bust of warrior* from La Cloche
558 suggests a Miocene age for the statuary limestone since this taxa has been reported in Provence
559 from the Aquitanian (Anglada et al., 1974) to the Burdigalian-Langhian (Descote, 2010). This
560 age together with the microfacies identified on thin sections (bryozoan-echinoderm grainstone-
561 packstone: **Fig. 6A-B**) rule out the hypothesis of a local origin (Barremian rudist-bearing
562 peloidal-foraminiferal packstone-grainstone: **Fig. 7C**). The light pinkish patina of the statue
563 leads to the hypothesis that the statuary material derives from La Couronne limestone
564 formation, late Burdigalian to early Langhian in age. Other Burdigalian limestones with similar
565 mechanical properties as La Couronne limestones crop out South of Martigues (Ponreau
566 Limestones) and are believed to have been used since the Antiquity as building stones (Tréziny,
567 2000). However, microfacies studies by Maurel-Ferrandini (1976) did not evidence bryozoan-
568 dominated pack-grainstones within the Ponreau section, thus excluding this provenance. To

569 validate such a hypothesis, a detailed petrographic and stable isotope study has been performed
570 on three sections located near La Couronne (**Fig. 1B** and **12**) across the Plan-de-Sausset (middle
571 Burdigalian) and La Couronne (late Burdigalian-early Langhian?) formations. Quantitative
572 analysis of grain composition of limestones revealed an excellent match between the statuary
573 material from La Cloche (bryozoan: 46%; echinoderms: 39%) and the bryozoan-dominated
574 limestones from the base of La Couronne formation (bryozoan: 45%; echinoderms: 41% in
575 COU06 sample) at the Anse du Verdon section. Such a correspondence is strongly confirmed
576 by carbon and oxygen stable isotope results (**Fig. 11B**): bulk $\delta^{13}\text{C}$ and $\delta^{18}\text{O}$ values measured
577 for La Cloche statue fall within the $\delta^{13}\text{C}$ - $\delta^{18}\text{O}$ domain of limestones from Anse du Verdon
578 section, while these are significantly outside the isotopic domains identified for Tamaris and
579 Beaumaderie sections. Such a lateral change in stable isotope signature within the Plan-de-
580 Sausset and La Couronne formations likely result from lateral changes in cementation and
581 neomorphic patterns from east to west. Interestingly, the stable isotope signature of La Cloche
582 statue is also extremely close to that of building stones from the Hellenistic Massalia harbor
583 (**Fig. 11 B**) which may support a common provenance, at the vicinity of Anse du Verdon and
584 La Couronne locality (see location **Fig. 2B**) or potentially further to the west (Carro). In
585 addition, the average estimated porosity values calculated from the different parts of the statue
586 (20.5%) is very close to that measured on outcrop samples from Baou Tailla (see location **Fig.**
587 **2B**), west of Anse du Verdon (20.4%). Complementing the existing petrographic and stable
588 isotope database by performing a systematic sampling in the whole set of identified ancient
589 quarries from La Couronne is likely to constrain even more the exact location of the extraction
590 site. Finally, our results show that the statue from La Cloche is made of a limestone whose place
591 of provenance is located approximately 19 km from the oppidum.

592

593 *5.1.3 The fragment of scapulary tunic from Baou de Saint-Marcel*

594 The clotted peloidal fabric, the dominant fenestral porosity as well as the encrustations around
595 plant stems allowed identifying the limestone from the Baou de Saint-Marcel statue as a
596 calcareous tufa. A local origin for the statuary limestone is therefore plausible since the Baou
597 de Saint-Marcel oppidum is located on top a hill composed of Pleistocene calcareous tufa,
598 displaying similar depositional fabrics (**Fig. 7D**). Additionally, the carbon and oxygen isotope
599 composition of the statuary limestone fall within the $\delta^{13}\text{C}$ and $\delta^{18}\text{O}$ range of Pleistocene
600 calcareous tufa from Provence, including samples from Baou de Saint-Marcel hill (**Fig. 11C**).
601 However, given the presence of various hills made up of calcareous tufa in the vicinity of the
602 Baou de Saint-Marcel oppidum (**Fig. 3D**) and more widely within the Marseille basin, the origin
603 of the statuary material could be not strictly local but located in other neighbouring continental
604 Pleistocene limestone outcrops from the Marseille basin (within 12 km from Baou de Saint-
605 Marcel).

606

607 *5.2 The Ziem Museum head: a regional or imported statue?*

608 One striking feature of the *male head* statue from the Ziem Museum is the dominance
609 of planktonic foraminifera, particularly *Heterohelix* whose stratigraphic distribution covers the
610 Upper Cretaceous and the Paleogene. The depositional facies of the Ziem Museum statue
611 suggests open marine environments. From the available literature, the only planktonic-rich
612 limestones known in Provence from the Upper Cretaceous-Paleogene interval occur in the
613 upper part of the Fontblanche formation (Fontblanche 2 unit: latest Cenomanian) in the
614 Beausset basin, 20 km southeast of Marseille (Rineau et al., 2021). From the available thin-
615 section database the closest depositional facies has been found in samples from the Collongues
616 slump (Fontblanche 2 unit: latest Cenomanian), 2 km north-east of Cassis (**Fig. 1A**). In these
617 samples, *Heterohelix* and *Hedbergella* dominate the biotic assemblage but the relative

618 frequency of glauconite and quartz grains differ very strongly from that of the Ziem Museum
619 statue. Additionally, no recent or ancient quarry is known in the Fontblanche 2 carbonate unit
620 since these rocks do not have the mechanical qualities required to be used as building stone or
621 sculpture because of their friability and disintegration into cm-thick plates. As a consequence,
622 with the current knowledge on carbonate rocks and stratigraphy of Provence, it seems unlikely
623 that the statuary limestone forming the Male Head from the Ziem Museum has a regional origin.
624 Its porosity estimate is low compared to the other studied statues.

625 The nearest outcrops of such planktonic-rich carbonates with dominant *Heterohelix* are
626 known in the Cenomanian-Turonian series from the Vocontian basin, southeast France (Oudet,
627 2013) and northern Africa (Morocco: Ettachfini and Andreu, 2004, Jati et al., 2011; Tunisia:
628 Saïdi et al, 1995), as well as around the Cretaceous-Tertiary boundary from northern Italy
629 (Luciani, 1997).

630 **5.3 Production of statuary limestone in protohistoric Provence**

631 The results of the integrative approach implemented in the present work provide strong
632 evidences that the three studied statues of Roquepertuse and that of Rognac are sourced from
633 the Lower Barremian, chalky limestones outcropping in the Massif de la Fare between Saint-
634 Chamas and Coudoux. The uniqueness and exact position of the stone production site are,
635 however, more questionable. The oolitic facies of the *twin-headed “Hermes”* and of the *seated*
636 *warrior* from Roquepertuse, becoming significantly rare towards Calissanne and passing
637 laterally into bioclastic grainstones (“Pierre de Calissanne”), leaves little doubt about the
638 location of the stone production site at the vicinity of Coudoux, thus confirming the intuition of
639 Gérin-Ricard (1927). Even though an ambiguity persists concerning the *Lintel with horses*
640 which displays a more ubiquitous bioclastic facies, present in both Coudoux and Calissanne
641 area, a common origin with the two other statues remains however to be privileged, taking into
642 account the greater distance from this last site compared to the oppidum (12 km compared to 4

643 km). The existence, on the hills north of Coudoux, of various ancient artisanal quarries (**Fig.**
644 **9C**), small in size (<10 m) and of undetermined period of activity, is consistent with past stone
645 extraction activity within the Coudoux limestone. The results of our study show that the
646 exploitation of the Coudoux limestone began as early as the 3rd century BC and possibly as
647 early as the last quarter of the 6th century BC if we take into account the ages of Roquepertuse
648 statuary suggested from stylistic approaches (Arcelin and Rapin, 2003).

649 The implications of the provenance analysis of La Cloche material on the production of
650 protohistoric statuary material are strongly dependent on the age attributed to the statue, which
651 remains controversial. If the age proposed by Arcelin and Rapin (2003), which is based on
652 stylistic analysis is confirmed, this would imply that La Couronne limestone was already
653 exploited at the vicinity of Anse du Verdon, and used for sculpture, as early as the end of the
654 3rd – 2nd century BC. This would suggest an early use of La Couronne limestone for sculpture
655 by Celto-Ligurians, prior to the earliest Greek massaliote settlements and associated Hellenistic
656 quarries documented near La Couronne (2nd century BC after Chausserie-Laprée, 2005) and
657 prior to the beginning of stone exportation toward the Massalia harbor (Pedini, 2009). While
658 superficial excavations of limestone slabs in the area have been reported as early as the 5th
659 century BC, earliest evidences of significant stone exploitations within the substrate of La
660 Couronne limestone are extractions of monolithic sills in the 4th century BC (Chausserie-
661 Laprée, 2005).

662 A later age for the bust of warrior from La Cloche, 1st century BC, as suggested by the
663 archaeological setting and stylistic considerations by Chabot (2005), would imply that the statue
664 was sculpted coevally with stone extraction by Greeks. Interestingly, the similarity in carbon
665 and oxygen stable isotope composition between the warrior from La Cloche and stones from
666 the fresh-water basin and southern tower of the hellenistic harbor of Massalia (2nd century BC)
667 suggests that these building materials likely derive from the same area as the statue, in the

668 vicinity of Anse du Verdon. Such a result is consistent with an extraction of the La Cloche
669 statuary limestone in a Hellenistic quarry. Additionally, such an interpretation would be also
670 consistent with the Massaliote affinity of the statue as attributed by Chabot (2005).

671 A transport by land of the statue across La Nerthe massif (~20 km) is possible since a
672 protohistoric winch press counterweight, made of La Couronne limestone, is known from the
673 Entremont oppidum (Coutagne, 1993) at a greater distance (~40 km) from the site of extraction.
674 However, a transport by sea of the statuary block from the coastal cliffs of La Couronne to the
675 Etang de Berre shoreline or to the Massalia harbour would have minimized the distance of land
676 transport (7 and 13 km respectively).

677 The early Pleistocene calcareous tufa (or *travertines*) from the Marseille basin are reputed to
678 been used as building stones or sculpture material since Antiquity (Vacca-Goutoulli, 2020).
679 Nicod (1974) mapped a set of ancient and recent quarries within the *travertines* from the eastern
680 districts of Marseille. Travertine blocks have been used in the Greek archaic construction
681 (Excavations of the Tunnel Major: Conche and Maufras, 2005) and in the reconstruction of the
682 ramparts at the 4th century BC (Treziny, 2009). Its use for sculpture is also attested during late
683 antiquity (Vacca-Goutoulli, 2020). The present results from Baou de Saint-Marcel material
684 indicate that the use of local *travertines* for sculpture started as early as the protohistoric times
685 in Segobrige territories east of Massalia.

686

687 **6. Conclusions**

688 An integrated approach including carbonate microfacies analysis, characterization of diagenetic
689 features and stable isotope geochemistry provided new insights into the provenance and the
690 production of statuary limestones in protohistoric Provence:

- 691 1) The *twin-headed “Hermes”*, the *lintel with horses* and the *warrior seated cross-legged*
692 from Roquepertuse are made of lower Barremian limestones from La Fare Massif, likely
693 from a same locality located at the vicinity of Coudoux, as suggested by a very close
694 analogy in micropalaeontologic markers (orbitolinids), grain size, texture and grain
695 composition (oolithic, oobioclastic and bioclastic grainstones), diagenetic features
696 (dissolution affecting ooid cortices) and stable isotope (carbon and oxygen) signatures.
697 Porosity values are also consistent with those measured in lower Barremian
698 microporous limestones from La Fare Massif. This also attests that the production of
699 Barremian limestones in La Fare Massif began as early as the 3rd century BC and
700 possibly earlier.
- 701 2) The *warrior seated cross-legged* from Rognac displays petrographic features
702 (occurrence of orbitolinids, bioclastic grainstone facies, development of perigranular
703 porosity) and stable isotope signatures which are consistent with a common provenance
704 with that of the Roquepertuse statues.
- 705 3) The bust of warrior from La Cloche oppidum is made of late Burdigalian-early Langhian
706 (?) limestones from La Couronne formation as suggested by the occurrence of
707 *Amphistegina* and the bryozoan-echinoderm biotic association. In addition, the carbon
708 and oxygen isotope composition strongly suggest a provenance from quarries located at
709 Anse du Verdon or possibly further to the west. This testifies the use of La Couronne
710 limestone in protohistoric sculpture (3rd to 1st century BC).
- 711 4) The fragment of *scapulary tunic* from Baou de Saint-Marcel revealed to be made of
712 local early Pleistocene calcareous tufa (=travertines), as suggested by the clotted-
713 peloidal and fenestral microfabric and the similar carbon and oxygen isotope signature.
714 This fragment records an early use of these limestones for protohistoric sculpture in
715 segobrige territories bordering Massalia.

716 5) The young *male head* from the Ziem Museum (Martigues) is made of a tight limestone
717 with planktonic foraminifera (*Heterohelix*) which indicate a late Cretaceous to
718 Paleogene age and for which no exact microfacies analogue exists in Provence. The site
719 of discovery as well as the stone provenance which is probably not located in Provence,
720 remain unknown.

721 The study therefore shows that for all the statues for which the place of discovery is certain,
722 the distance to the site of provenance of the limestone is less than 20 km. Finally, from a
723 methodological point of view, this work demonstrates the potentiality of integrating detailed
724 microfacies, diagenetic and stable isotope analyzes of carbonate rocks for determining the
725 provenance of statuary limestones. However, the success of such an approach lies mainly on
726 the existence of substantial petrographic and geochemical databases on a regional scale. On
727 the other hand, the tested in situ non-invasive techniques proved to be inapplicable for the
728 studied limestones. Provenancing of limestone statues is seldom reported (e.g. Middleton and
729 Bradley, 1989), probably because such rocks are so common that comparison techniques are
730 tedious. In the present case we benefited a lot from the existing petrographic, paleontologic
731 and isotopic databases on Provence limestones.

732

733 **Acknowledgement**

734 This work was supported by a Master student grant (Adam Ouass, CEREGE, Aix-Marseille
735 Université) from the Marseille Municipality (Ville de Marseille). We are grateful to Yann
736 Ternois (CEREGE), Véronique Rinalducci (LA3M) and Lionel Roux (LA3M) for their
737 technical support for photogrammetric acquisition.

738

739 **References**

740

741 Agostini, P., 1972. L'oppidum préromain des Baou de Saint-Marcel à Marseille (VIIe-IIe s.).

742 PhD thesis, Aix-Marseille University, 145 p.

743 Anglada, R., Arnaud, M., Catzigras, F., Colomb, E., Delcourt, A., Ferrandini, M., 1974. Etude

744 stratigraphique et sédimentologique de l'Aquitaniens de la Calanque du Petit Nid (Sausset,

745 Bouches-du-Rhône, France). Découverte d'un squelette d'*Halitherium* Kaup. *Géologie*

746 *Méditerranéenne*, 1, 1-7.

747 Arcelin, P., Rapin, A., 2003. L'iconographie anthropomorphe de l'âge du Fer en Gaule

748 méditerranéenne. In: Décors, images et signes de l'âge du Fer européen, XXVIe colloque de

749 l'AFEAF, thème spécialisé. Tours : Fédération pour l'édition de la Revue archéologique du

750 Centre de la France, p. 183-219.

751 Attanasio, D., Armiento, G., Brilli, M., Emanuele, M.C., Platania, R., Turi, B., 2000.

752 Multimethod marble provenance determinations: the Carrara marbles as a case study for the

753 combined use of isotopic, electron spin resonance and petrographic data. *Archaeometry* 42,

754 257-272.

755 Aubert, I., Léonide, P., Lamarche, J., Salardon, R., 2020. Diagenetic evolution of fault zones in

756 Urgonian microporous carbonates, impact on reservoir properties (Provence – southeast

757 France). *Solid Earth*, 11, 1163-1186.

758 Babinot, J.-F., Tronchetti, G., 1983. Les microfaunes (foraminifères -ostracodes) du Coniacien

759 -Santonien de Provence (S.E. France) : biostratigraphie, paléoécologie. *Géologie*

760 *Méditerranéenne*, 10, 3-4, 143-154.

761 Boissinot, P., 2011. Stèles et statues de Roquepertuse : état de la question. *Documents*

762 *d'Archéologie Méridionale*, 34, 247-262.

763 Boissinot, P., Gantès, L.-F., Gassend, J.-M., 2000. La chronologie de Roquepertuse.
764 Propositions préliminaires à l'issue des campagnes 1994-1999. *Documents d'Archéologie*
765 *Méridionale*, 23, 249-271.

766 Borgomano, J., Masse, J.-P., Fenerci-Masse, M., Fournier, F., 2013. Petrophysics of Lower
767 Cretaceous platform carbonate outcrops in Provence (SE France): implications for carbonate
768 reservoir characterisation. *Journal of Petroleum Geology*, 36 (1), 5–42.

769 Boudagher-Fadel, M., Price, G.D., 2019. Global evolution and paleogeographic distribution of
770 mid-Cretaceous orbitolinids. *UCL Open: Environment*, 1, 01. 21p.

771 Brillì, M., Conti, L., Giustini, F., Occhiuzzi, M., Pensabene, P., De Nuccio, M., 2011.
772 Determining the provenance of black limestone artifacts using petrography, isotopes and EPR
773 techniques: the case of the monument of Bocco. *Journal of Archaeological Science*, 38, 1377-
774 1384.

775 Brunier, G., Fleury, J., Anthony, E.-J., Gardel, A., Dussouillez, P., 2016, Close-range airborne
776 Structure-from-Motion Photogrammetry for high-resolution beach morphometric surveys:
777 Examples from an embayed rotating beach. *Geomorphology*, 261, 76-88.

778 Capedri, S., Venturelli, G., De Maria, S., Mantovani Uguzzoni, M. P., and Pancotti, G., 2001,
779 Characterisation and provenance of stones used in the mosaics of the Domus dei Coiedii at
780 Roman Suasa (Ancona, Italy), *Journal of Cultural Heritage*, 2, 7–22.

781 Chabot, L., 1983. L'oppidum de la Cloche aux Pennes-Mirabeau (Bouches-du-Rhône) :
782 Synthèse des travaux effectués de 1967 à 1982. *Revue Archéologique de Narbonnaise*, 16, 39-
783 80.

784 Chabot, L., 1996. Une aire culturelle sur l'oppidum de La Cloche aux Pennes-Mirabeau
785 (Bouches-du-Rhône). Les enseignements de la zone sommitale. *Revue Archéologique de*
786 *Narbonnaise*, 29, 233-278.

787 Chabot, L., 2005. Notice 19, La Cloche, In : M.-P. Rothé and H. Tréziny (Eds), Carte
788 Archéologique de la Gaule - Marseille et ses alentours, 13/3, pp. 839-849.

789 Chausserie-Laprée, J., 2002. Martigues. Les carrières de La Couronne-Carro : la carrière de
790 *Baou Tailla*. In : Bilan scientifique DRAC-PACA, SRA, 2002, p. 121-125.

791 Chausserie-Laprée, J., 2005. Martigues, terre gauloise. Entre Celtique et Méditerranée. Paris,
792 Errance, 251 p.

793 Clerc, M., 1914. Note sur un fragment de statue trouvé à Rognac (Bouche-du-Rhône). *Revue*
794 *des Études Anciennes*, 16, 1, 81-82.

795 Conche F., Maufras, O., 2005. Notice 83, Tunnel de la Major, In : M.-P. Rothé and H. Tréziny
796 (Eds), Carte Archéologique de la Gaule - Marseille et ses alentours, 13/3, pp. 428-453.

797 Coutagne, D., 1993. Archéologie d'Entremont, Musée Granet. Association du Musée Granet
798 and Association Archéologie d'Entremont, 263 p.

799 Dedet, B., Gantès, L.-F., 2014. Ensevelissements de nouveau-nés et traces de pratiques
800 culturelles gauloises sur l'habitat du Baou de Saint-Marcel, aux portes de Marseille grecque.
801 *Documents d'Archéologie Méridionale*, 37, 73-88.

802 Deocampo, D.M., 2009. The geochemistry of continental carbonates. In: Alonso-Zarza, A.M.,
803 Tanner, L.H. (Eds), Carbonates in Continental Settings: Geochemistry, Diagenesis and
804 Settings. *Developments in Sedimentology*, 62, 336 p.

805 Descote, P.Y., 2010. Relations architecturales, faciologiques et diagénétiques des carbonates
806 bioclastiques du bassin miocène rhodano-provençal (SE France). PhD thesis, École Nationale
807 Supérieure des Mines de Paris, 147p.

808 D'Ovidio, A.-M., Rothé M.-P., 2005. Notice 278, Baou de Saint-Marcel, In : M.-P. Rothé and
809 H. Tréziny (Eds), Carte Archéologique de la Gaule - Marseille et ses alentours, 13/3, pp. 699-
810 716.

811 Duceppe-Lamarre, A., 2002. Unité ou pluralité de la sculpture celtique hallstattienne et
812 laténienne en pierre en Europe continentale du VIIe au Ier s. av. J.-C. *Documents d'archéologie*
813 *méridionale*, 25, 285-318.

814 Ettachfini, M., Andreu, B., 2004. Le Cénomaniens et le Turonien de la Plate-forme Préafricaine
815 du Maroc. *Cretaceous Research*, 25 (2), 277-302.

816 Flügel, E., and Flügel, C., 1997, Applied microfacies analysis: provenance studies of Roman
817 mosaic stones, *Facies*, 37, 1–48.

818 Frahm, E.; Feinberg, J. M. From Flow to Quarry: Magnetic Properties of Obsidian and Changing
819 the Scale of Archaeological Sourcing. *J. Archaeol. Sci.* 2013, 40 (10), 3706–3721.

820 Frey, O.-H., Hermann, F.-R, 1997. Ein frühkeltischer Fürstengrabhügel am Glauberg im
821 Witteraukreis, Hessen. *Germania*, 75/2, 459-550.

822 Gérin-Ricard, 1927. Le sanctuaire préromain de Roquepertuse à Velaux (Bouches-du-Rhône):
823 son trophée, ses peintures, ses sculptures, étude sur l'art Gaulois avant les temps classiques.
824 Société de Statistique, d'Histoire et d'Archéologie de Marseille et de Provence, 53 p.

825 Guichard, C., Rayssiguier, G., 1993. Les Baou de Saint-Marcel à Marseille. Etude
826 stratigraphique du secteur III (VIe-IIe siècles avant J.-C.). *Documents d'Archéologie*
827 *Méridionale*, 16, 231-256.

828 Jati M., Grosheny D., Ferry S., Masrour M., Aoutem M., Içame N., Gauthier Lafaye F., and
829 Desmares D., 2011. The Cenomanian-Turonian boundary event on the Moroccan Atlantic
830 margin (Agadir basin): Stable isotope and sequence stratigraphy. *Paleogeography,*
831 *Paleoclimatology, Paleoecology*, 296, 151-164.

832 Léonide, P., Fournier, F., Reijmer, J.J.G., Vonhof, H., Borgomano, J., Dijk, J., Rosenthal, M.,
833 van Goetem, M., Cochard, J., Meulenaars, K., 2014. Diagenetic patterns and pore space
834 distribution along a platform to outer-shelf transect (Urgonian limestone, Barremian-Aptian,
835 SE France). *Sedimentary Geology*, 306, 1-23.

836 Lescure, B., Werth, F., 2000. Provenance des matières premières utilisées dans la statuaire de
837 Roquepertuse (Velaux, Bouches-du-Rhône). Analyses physico-chimiques. *Revue*
838 *Archéologique de Narbonnaise*, 33, 273-274.

839 Luciani, V., 1997. Planktonic foraminiferal turnover across the Cretaceous-Tertiary boundary
840 in the Vajont valley (Southern Alps, northern Italy). *Cretaceous Research*, 18, 799–821.

841 Maurel-Ferrandini, M., 1976. Reconstitution paléogéographique du Burdigalien du littoral de
842 la chaîne de La Nerthe et de la région des Etangs (B. du Rhône, France). *Travaux du*
843 *Laboratoire de Géologie Historique et de Paléontologie*, 7, 132 pp.

844 Mellinand, P., Saget-Basseuil, E., Brousse, S., Chevillot, P., Corré, X., Delpalillo, D.,
845 Dumas, V., Gantès, L.-F., Guillon, O., Hadot, V., Jaccottey, L., Lang-Desvignes, S., Moliner,
846 M., D'ovidio, A.-M., Pawlowicz, M., Tréziny, H., Vallet, J.-M., 2021. Port antique à Marseille
847 (Bouches-du-Rhône) : surveillance archéologique des travaux de requalification. Rapport de
848 fouille. Dossier 12161, Inrap Midi-Méditerranée. 276 pp.

849 Menez, Y., Giot, P.-R., Laubenheimer, F., Le Goff, E., Vendries, C., 1999. Les sculptures
850 gauloises de Paule (Côtes d'Armor). *Gallia*, 56, 1999, pp. 357-414.

851 Middleton, A.P. and Bradley, S.M., 1989. Provenancing of Egyptian limestones sculptures. *J.*
852 *Archeol. Sci.* 16 (5), 475-488.

853 Nicod, J., 1974. Site et urbanisation dans la banlieue résidentielle Est de Marseille.
854 *Méditerranée*, 18, 3, 127-133.

855 Oudet, C., 2013. Evolution des associations de foraminifères comme bioindicateurs des paléo-
856 environnements : le bassin subalpin (bassin vocontien et sa marge occidentale) au Cénomanién.
857 PhD thesis, University of Strasbourg, 259p.

858 Pédini, C., 2009. Exploitation et utilisation du calcaire de La Couronne dans l'Antiquité
859 (Martigues, Bouches-du-Rhône. *Revue Archéologique de Narbonnaise*, 42, 265-287.

860 Pédini, C., 2013. *Les carrières de la Couronne de l'Antiquité à l'époque contemporaine*.
861 Errance, Centre Camille Jullian, 316 p.

862 Py, M., 2011. La sculpture gauloise méridionale. Paris, Errance 2011, 200 p.

863 Rapin, A., 2004. Pour une nouvelle lecture de la sculpture préromaine de Gaule méridionale.
864 In : P. Arcelin (P.) and G. Congès, Eds. –La sculpture protohistorique de Provence dans le Midi
865 gaulois, *Documents d'Archéologie Méridionale*, 23, 13-22.

866 Rayssiguier, G. 1989. Marseille. Baou de Saint-Marcel. Dépôt d'objets métalliques - Deuxième
867 moitié du VIe s. av. J.-C. Direction des Antiquités de la Région Provence - Alpes - Côte d'Azur,
868 Notes d'Information et de Liaison, 6, 102-103.

869 Rayssiguier, G., Guichard, C., 1989. Un dépôt d'objets métalliques aux Baou de Saint-Marcel
870 à Marseille. *Documents d'Archéologie Méridionale*, 12, 245-251.

871 Rineau, V., Floquet, M., Villier, L., Léonide, P., Blénet, A., Ackouala Mfere, A.-P., 2021.
872 Ecological successions of rudist communities: A sedimentological and palaeoecological
873 analysis of upper Cenomanian rudist assemblages from the South-Provence Carbonate Platform
874 (SE France). *Sedimentary Geology*, 421, 105964.

875 Rochette, P., Ambrosi, J.P., Amraoui, T., Andrieu, V., Badie, A., Borgard, P., Gattacceca, J.,
876 Hartmann-Virnich, A., Panneau, M., Planchon, J., 2022. Systematic sourcing of granite shafts

877 from Gallia Narbonensis and comparison with other western Mediterranean areas. *J. Archo.*
878 *Sc. Rep.*, 42, 103372.

879 Saïdi, F., Ben Ismaïl, M.H., Negra, M.H., M'Rabet, A., 1995. La plate-forme carbonatée
880 cénomaniennne de Tunisie du Centre-Ouest. Faciès, cortèges argileux, paléoenvironnements et
881 stratigraphie séquentielle. *Géologie Méditerranéenne*, 22 (1), 17-41.

882 Sanmarco, M., Margiotta, S., Foresi, L. M., Ceraudo, G., 2015. Characterization and
883 provenance of building materials from the Roman Pier at San Cataldo (Lecce, southern Apulia,
884 Italy): a lithostratigraphical and micropaleontological approach. *Mediterranean Archaeology*
885 *and Archaeometry*, 15, 2, 101-112.

886 Tréziny, H., 2000. La pierre de construction des remparts antiques de Marseille. *Revue*
887 *Archéologique de Narbonnaise*, 33, 275-278.

888 Tréziny, H. 2009. La pierre de construction à Marseille de l'Antiquité aux Temps modernes,
889 In : P. Jockey Ed., Λευκός λίθος : marbres et autres roches de la Méditerranée antique: études
890 interdisciplinaires, Association for the Study of Marble and Other Stones Used in Antiquity
891 (ASMOSIA), Collection l'Atelier méditerranéen, Paris, p. 203–212.

892 Triantafyllou, A., Mattielli, N., Clerbois, S., 2021. Optimizing multiple non-invasive
893 techniques (PXRF, pMS, IA) to characterize coarse-grained igneous rocks used as building
894 stones. *Journal of Archaeological Science* 129, 15, 105376.

895 Uchida E., Watanabe, R. Cheng, R., Nakamura, Y., Takeyama, T., 2021. Non-destructive in-
896 situ classification of sandstones used in the Angkor monuments of Cambodia using a portable
897 X-ray fluorescence analyzer and magnetic susceptibility meter. [Journal of Archaeological](#)
898 [Science: Reports](#) 39, 103137.

899 Vacca-Goutoulli, M., 2020. L'approvisionnement des matériaux de la sculpture en calcaire à
900 Marseille dans l'Antiquité: l'origine et la pertinence de ce choix à travers l'étude des
901 caractéristiques physiques des différents calcaires régionaux. Leur interprétation dans le rendu
902 plastique de l'œuvre. In : H. Aurigny and V. Gaggadis-Robin Eds., Nouvelles recherches sur la
903 sculpture en calcaire en Méditerranée, Centre Camille Jullian, p. 15-42.

904 Virgone, A., 1997. Stratigraphie, sédimentologie et dynamique d'une plate-forme carbonatée: le
905 Berriasien supérieur-Valanginien basal de Basse-Provence occidentale (S.E. France. PhD
906 thesis, Université de Provence, Marseille, 196 p.

907 Williams-Thorpe, O., 2008. A thousand and one columns: observations on the Roman granite
908 trade in the Mediterranean area. *Oxford Journal of Archaeology* 27, 73-89.

909

910

911 **Figure caption**

912 **Fig.1: A-G:** Photographs of the studied set of protohistoric statues: **A)** *warrior seated cross-*
913 *legged* (Roquepertuse), Musée d'Histoire de Marseille (MHM), **B)** *lintel with horses*
914 (Roquepertuse), MHM, **C)** *twin-headed "Hermes"* (Roquepertuse), MHM, **D)** *warrior seated*
915 *cross-legged* (Plan des Clapiers, Rognac), MHM, **E)** *bust of warrior* (La Cloche), MHM, **F)**
916 *Fragment of scapulary tunic* (Baou de Saint-Marcel), MHM, **G)** *Young male head*, Ziem
917 *Musem.* **H)** Photogrametric image of the *twin-headed "Hermes"* (Roquepertuse), MHM.

918 **Fig.2: A)** Simplified geological map of Provence and location of the places of discovery of the
919 studied statues. **B)** Close-up on La Couronne area and location of the studied sections and
920 position of ancient quarries (after Pedini, 2013).

921 **Fig. 3:** Geological map around the places of discovery of the protohistoric statues: **A)** Velaux
922 and Roquepertuse oppidum, **B)** Rognac and Le Castellas oppidum: the yellow star locates the
923 place of discovery of the warrior seated cross-legged (Plan du Clapier), **C)** La Cloche oppidum,
924 **D)** Baou de Saint-Marcel oppidum.

925 **Fig. 4:** Petrographic features of the *twin-headed "Hermes"* from Roquepertuse: **A)** thin-section
926 microphotograph under polarized light showing the oolitic grainstone facies (BF1); Orb.:
927 Orbitolinid, white arrows: ooids; **B-C)** close up on ooids showing the dissolution of the cortex
928 and partial infill with equigranular sparry calcite under polarized (**B)** and polarized-analyzed
929 light (**C**); **D-E)** SEM images of an ooid; *Pal.:* isopachous palissage calcite cement; *Equ.:*
930 equigranular sparry calcite crystal occupying the dissolution void within the cortex of the ooid;
931 *Bl.:* blocky calcite cement.

932 **Fig. 5:** Petrographic features of **A-B-C)** the *warrior seated cross-legged* from Roquepertuse,
933 **D-E)** the *lintel with horses* from Roquepertuse and **F-G)** the *warrior seated cross-legged* from
934 Rognac. **A)** thin section microphotograph under polarized light showing the oo-bioclastic

935 grainstone facies (BF2); white arrows: ooids; **B-C**) close up on ooids showing the dissolution
936 of the cortex and partial infill with equigranular sparry calcite under polarized; **D** and **F**) thin
937 section microphotograph under polarized light showing the bioclastic grainstone facies (BF3),
938 *Orb.*: Orbitolinid; **E** and **G**) SEM images; black arrows: dissolution features around grains,
939 white arrows: partially preserved intergranular pores.

940 **Fig. 6: A-B**) *Bust of warrior* from La Cloche: thin section microphotograph under polarized
941 light showing the bioclastic packstone-grainstone dominated by bryozoan (Bryo.) and echinoids
942 (Ech.); *Amph.*: *Amphistegina*; **C-D**): fragment of scapulary tunic from Baou de Saint-Marcel:
943 thin section microphotograph under polarized light showing the clotted peloidal microfabric;
944 white arrow: calcitic encrustation around plant stem; **E-G**) The *male head* from Ziem Museum:
945 thin section microphotograph under polarized light showing the planktonic foraminiferal
946 packstone (white arrow: sections of planktonic foraminifers); **F**) SEM image of a section of
947 *Heterohelix*; **G**) SEM image showing fragmented coccoliths (white arrow) within the micrite
948 matrix.

949 **Fig.7:** Thin section microphotograph under polarized light of outcrop samples: **A**) local
950 limestone from Roquepertuse oppidum (“Calcaire de Rognac” formation, latest Campanian to
951 earliest Maastrichtian); *rt*: root traces, *pis.*: vadose pisoids; **B**) local limestone from Castellas
952 oppidum (“Calcaire de Rognac”, latest Campanian to earliest Maastrichtian), *gyr.*: characean
953 gyrogonite, *rt*: root traces; **C**) local limestone from La Cloche oppidum (Barremian, Urgonian
954 facies), *Orb.*: orbitolinid, **mil.**: miliolids; *Ech.*: echinoderms; **D**) local limestone from Baou de
955 Saint-Marcel oppidum, calcareous tufa (early Pleistocene) with calcite encrustations around
956 stems (arrow), **E**) Planktonic-dominated packstone from the Collongues slump, north-east of
957 Cassis (Fontblanche 2 formation, latest Cenomanian), *pf*: planktonic formainifer, *Qz*: quartz
958 grain, *gl.*: glauconite.

959 **Fig.8:** **A)** $\delta^{13}\text{C}$ - $\delta^{18}\text{O}$ cross-plot for statuary and local limestones, **B)** $\delta^{13}\text{C}$ - $\delta^{18}\text{O}$ cross-plot for
960 the regional limestone database.

961 **Fig. 9:** **A)** Textural log and vertical facies changes of the upper part of Lower Barremian
962 succession, north of Coudoux (see location in **B** and **C**); **B)** Geological map of the southern
963 flank of La Fare Massif, north of Coudoux and position of the section logged in **A**; **C)** Aerial
964 view of the logged section and position of abandoned quarries.

965 **Fig.10:** **A)** Thin section microphotograph of sample COU-A from Coudoux section, showing
966 the oolitic grainstone facies (BF1) and comparison of carbonate grain composition between
967 COU-A and the *twin-headed "Hermes"* from Roquepertuse; **B)** Thin section microphotograph
968 of sample COU-B from Coudoux section, showing the oobioclastic grainstone facies (BF2) and
969 comparison of carbonate grain composition between COU-B and the *warrior seated cross-*
970 *legged* from Roquepertuse; **C)** Thin section microphotograph of sample COU-C from Coudoux
971 section, showing the bioclastic grainstone facies (BF1) and comparison of carbonate grain
972 composition between COU-A, the *lintel with horses* from Roquepertuse and the *warrior seated*
973 *cross-legged* from Rognac; **D)** Detail of an ooid with leached cortex and equigranular sparry
974 calcite infill, under polarized (left) and polarized-analyzed light (right), COU-A sample,
975 Coudoux.

976 **Fig. 11:** $\delta^{13}\text{C}$ - $\delta^{18}\text{O}$ cross-plots: **A)** Statuary limestones from Roquepertuse and Rognac and
977 regional Barremian limestones; **B)** Bust of warrior from La Cloche and regional Burdigalian-
978 early Langhian (?) limestones ("Pierre de la Couronne"); **C)** Fragment of scapulary tunic from
979 Baou de Saint-Marcel and regional Pleistocene calacareous tufa.

980 **Fig.12:** **A)** Log section of La Couronne/Anse du Verdon (see location in **Fig. 1B**) and bioclastic
981 composition of limestones determined from point counting on thin-section; **B)** Photograph of
982 the outcrop (eastern coast of Anse du Verdon) showing the upward transition from Plan de

983 Sausset (Middle Burdigalian) and La Couronne (Upper-Burdigalian-early Langhian?)
984 formation and the position of ancient quarries on top; **C)** Comparison of microfacies and grain
985 composition between COU6 sample from La Couronne and the *bust of warrior* from La Cloche;
986 Bryo: bryozoan; Ech.: echinoderms.

987

988 **Table 1:** Thin-section database of limestones from Provence.

989

990 **Table 2:** Carbon and oxygen isotope database of selected limestones from Provence.

991

992 **Table 3:** Results of non-destructive methods: pXRF measurements using Bruker instrument
993 expressed as ratio to CaO or Ca content (in ‰), density and porosity estimates.

994

995 **Appendix:** Carbon and oxygen isotope measurements

FIGURE 1

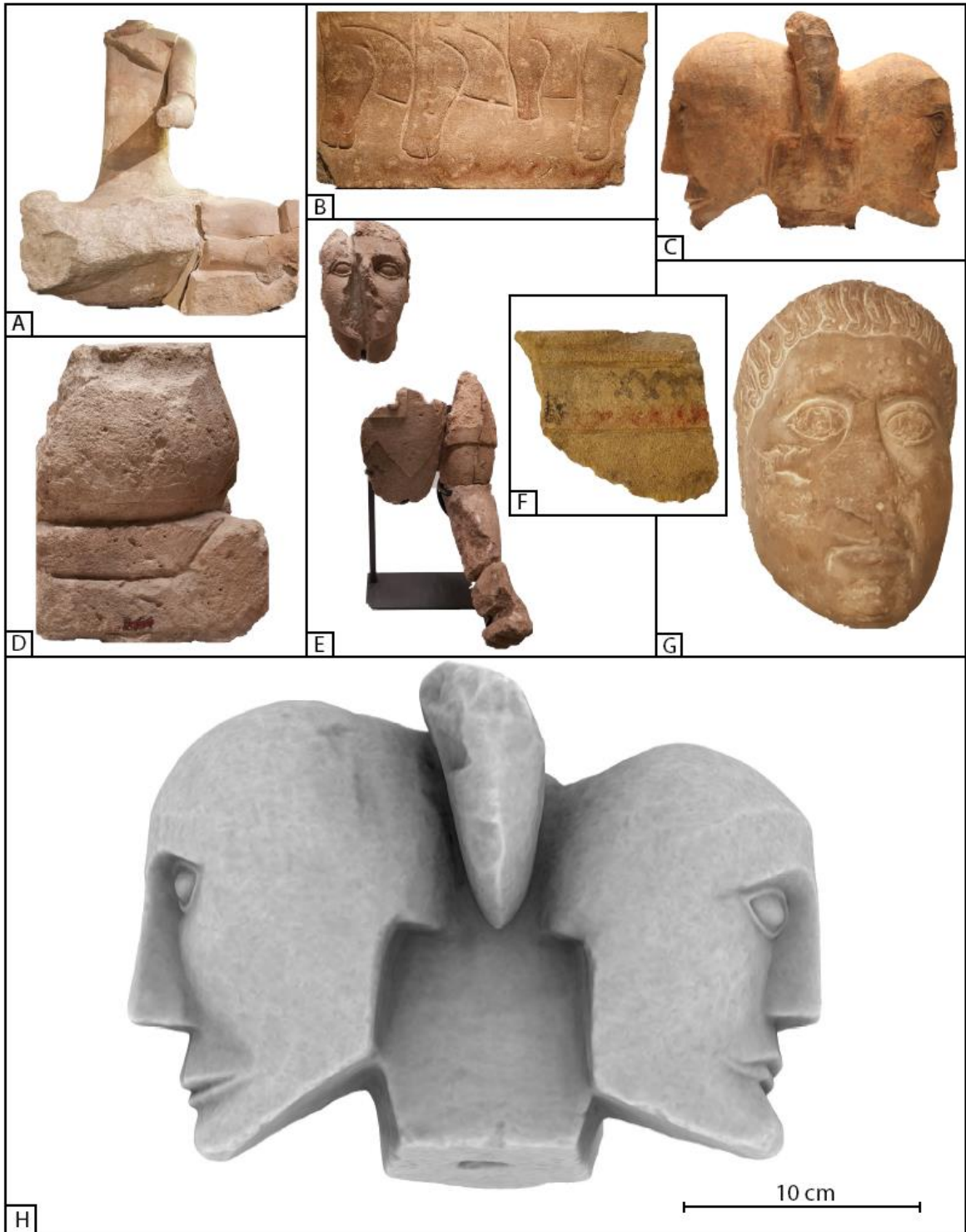


Figure 1: A-G: Photographs of the studied set of protohistoric statues: **A)** *warrior seated cross-legged* (Roquepertuse), Musée d'Histoire de Marseille (MHM), **B)** *lintel with horses* (Roquepertuse), MHM, **C)** *twin-headed "Hermes"* (Roquepertuse), MHM, **D)** *warrior seated cross-legged* (Plan des Clapiers, Rognac), MHM, **E)** *bust of warrior* (La Cloche), MHM, **F)** *Fragment of scapulary tunic* (Baou de Saint-Marcel), MHM, **G)** *Young male head*, Ziem Musem. **H)** *Photogrammetric image of the twin-headed "Hermes"* (Roquepertuse), MHM.

FIGURE 2

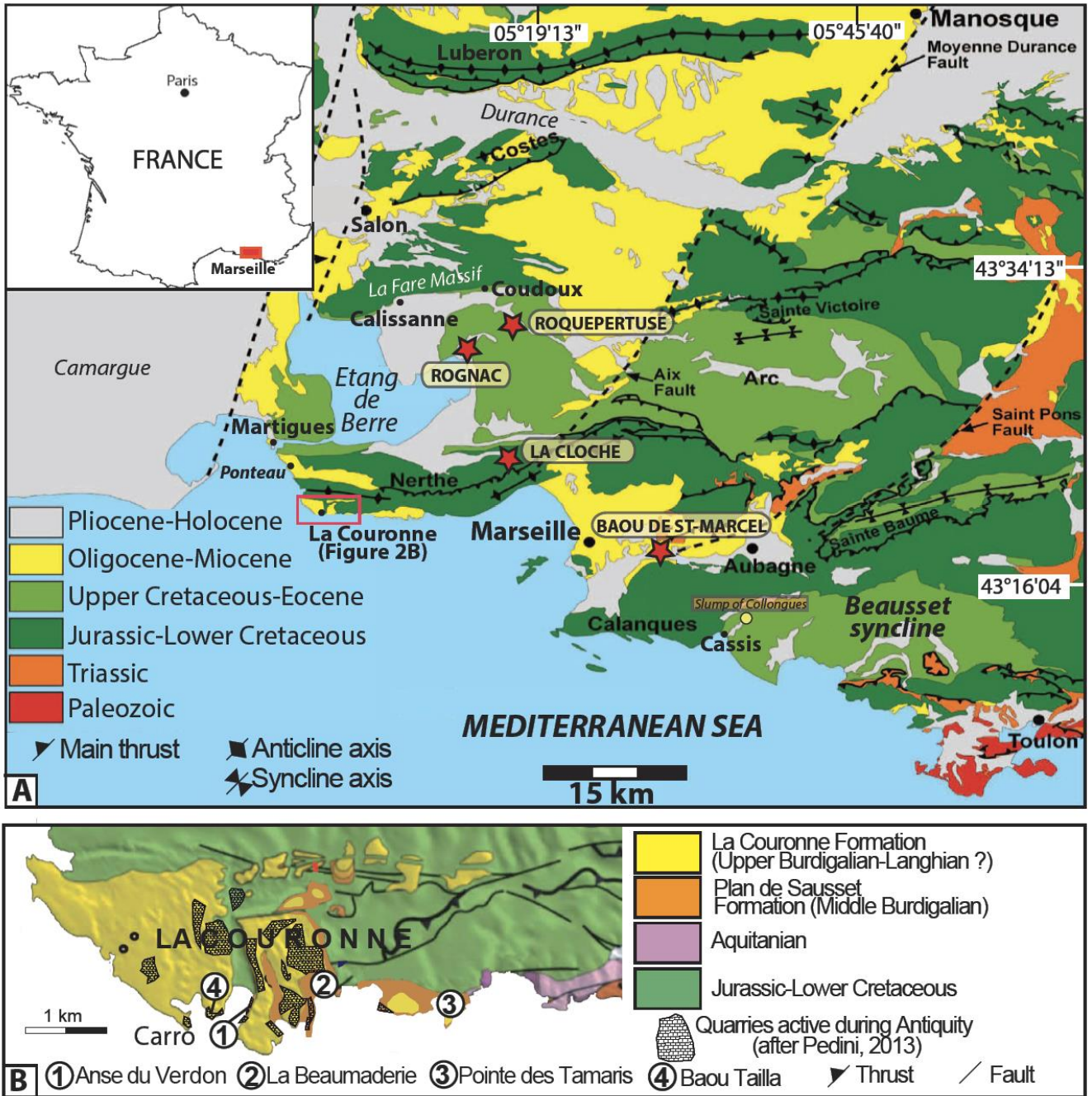


Figure 2: A) Simplified geological map of Provence and location of the places of discovery of the studied statues. **B)** Close-up on La Couronne area and location of the studied sections and position of ancient quarries (after Pedini, 2013).

FIGURE 3

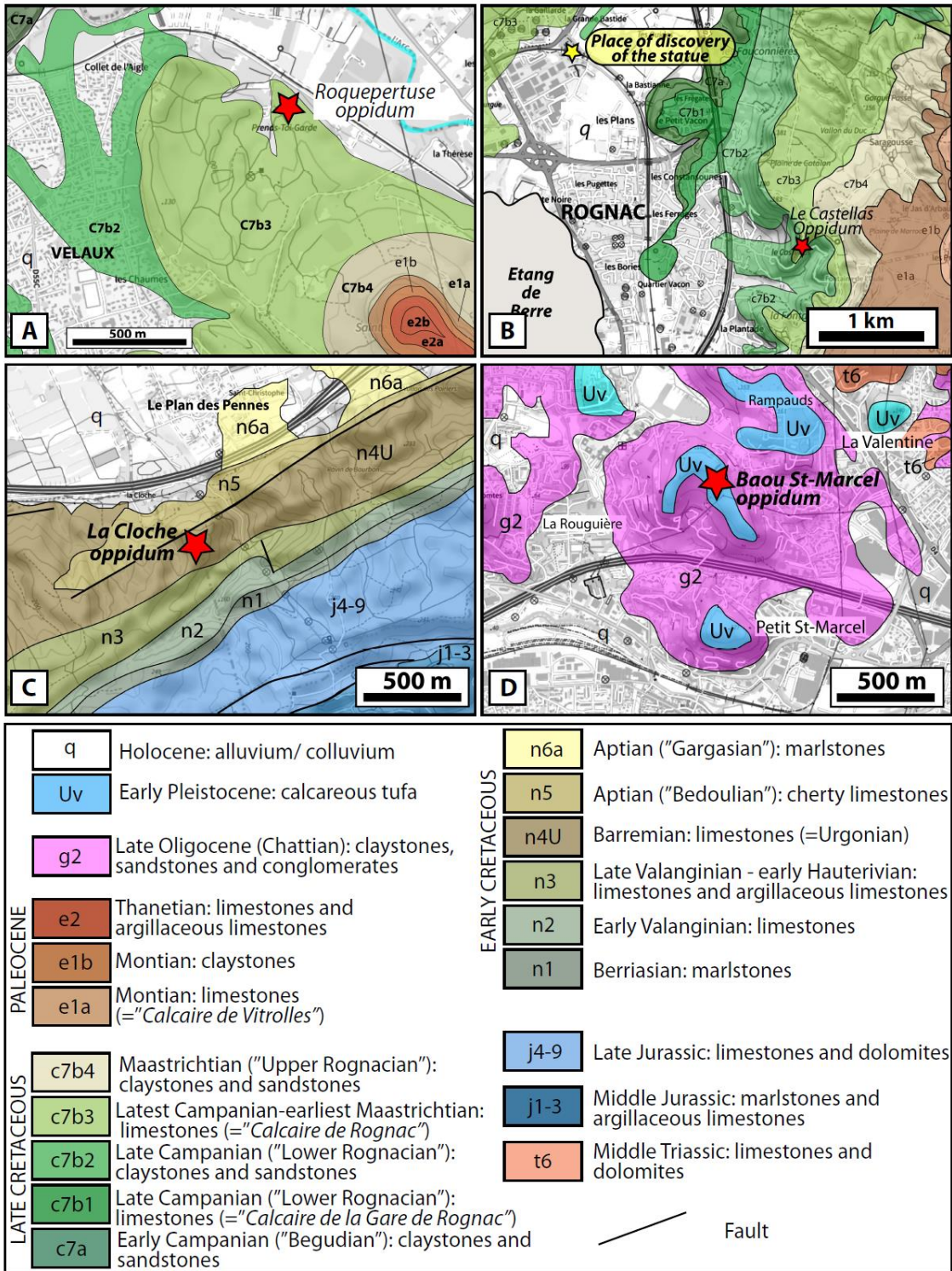


Figure 3: Geological map around the places of discovery of the protohistoric statues: **A)** Velaux and Roquepertuse oppidum, **B)** Rognac and Le Castellàs oppidum: the yellow star locates the place of discovery of the warrior seated cross-legged (Plan du Clapier), **C)** La Cloche oppidum, **D)** Baou de Saint-Marcel oppidum.

FIGURE 4

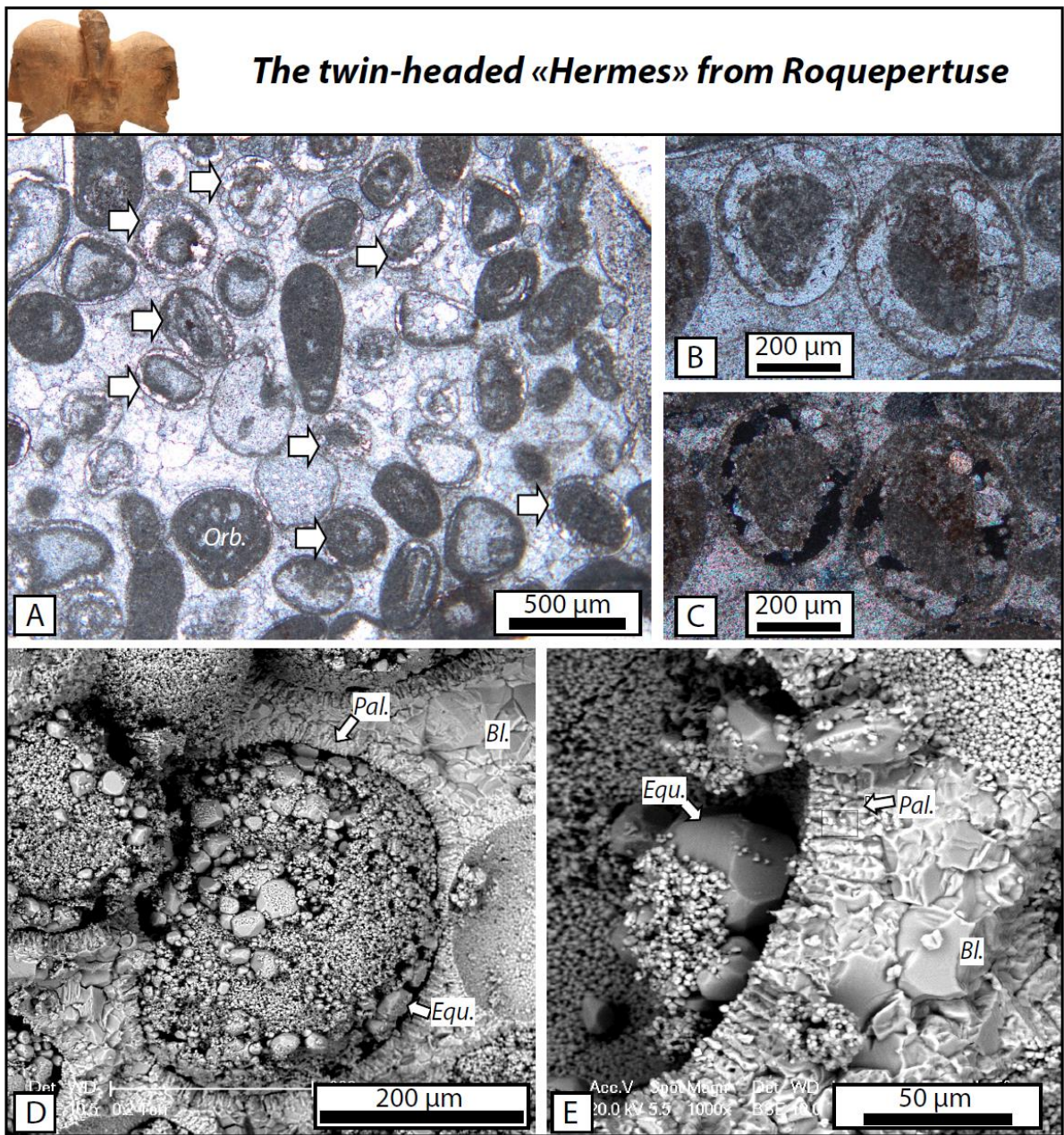


Figure 4: Petrographic features of the *twin-headed* “Hermes” from Roquepertuse: **A)** thin-section microphotograph under polarized light showing the oolitic grainstone facies (BF1); Orb.: Orbitolinid, white arrows: ooids; **B-C)** close up on ooids showing the dissolution of the cortex and partial infill with equigranular sparry calcite under polarized (**B**) and polarized-analyzed light (**C**); **D-E)** SEM images of an ooid; *Pal.*: isopachous palissage calcite cement; *Equ.*: equigranular sparry calcite crystal occupying the dissolution void within the cortex of the ooid; *Bl.*: blocky calcite cement.

FIGURE 5

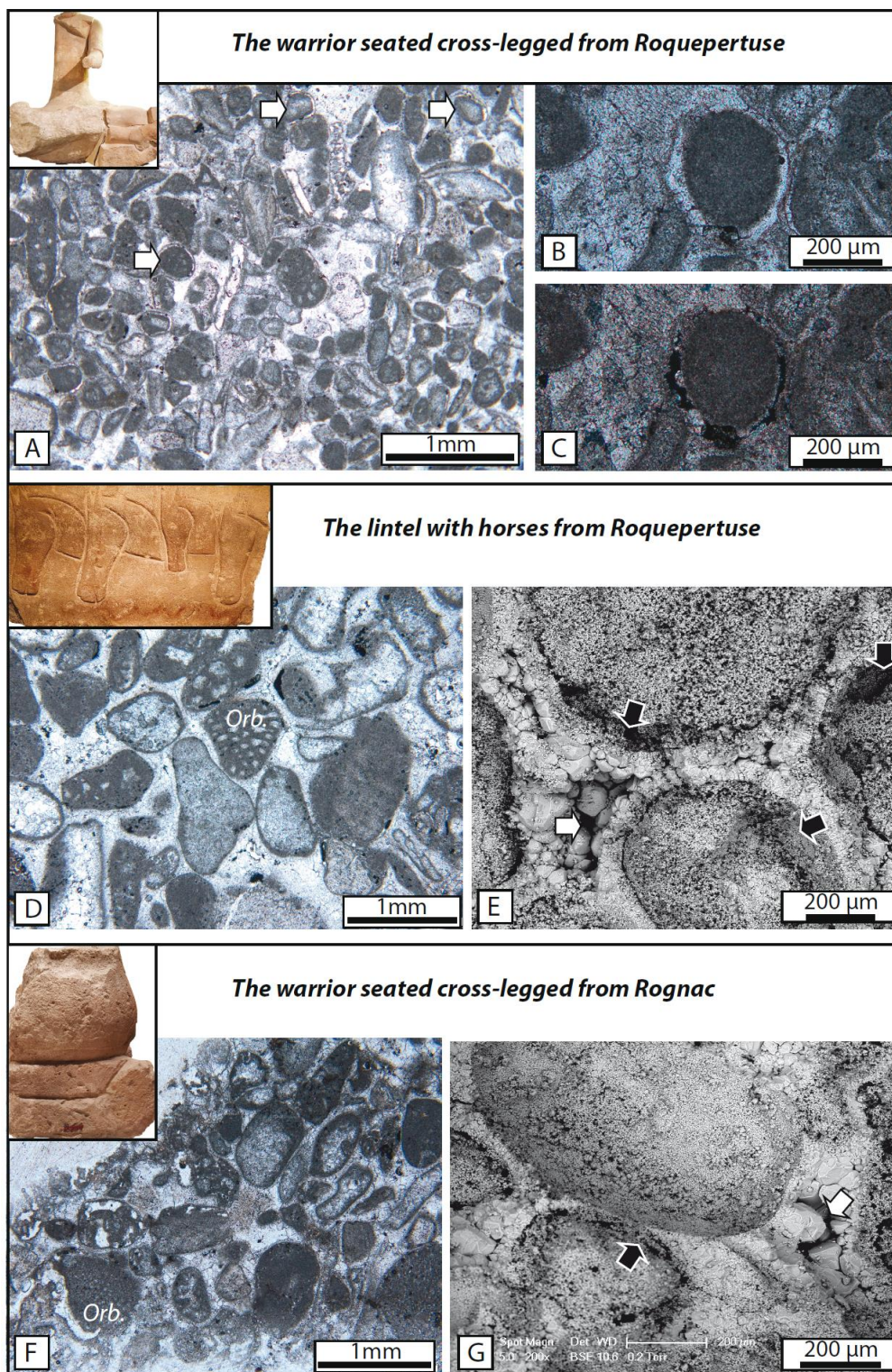


Figure 5: Petrographic features of **A-B-C**) the *warrior seated cross-legged* from Roquepertuse, **D-E**) the *lintel with horses* from Roquepertuse and **F-G**) the *warrior seated cross-legged* from Rognac. **A**) thin section microphotograph under polarized light showing the oo-bioclastic grainstone facies (BF2); white arrows: ooids; **B-C**) close up on ooids showing the dissolution of the cortex and partial infill with equigranular sparry calcite under polarized; **D** and **F**) thin section microphotograph under polarized light showing the bioclastic grainstone facies (BF3), *Orb.*: Orbitolinid; **E** and **G**) SEM images; black arrows: dissolution features around grains, white arrows: partially preserved intergranular pores.

FIGURE 6

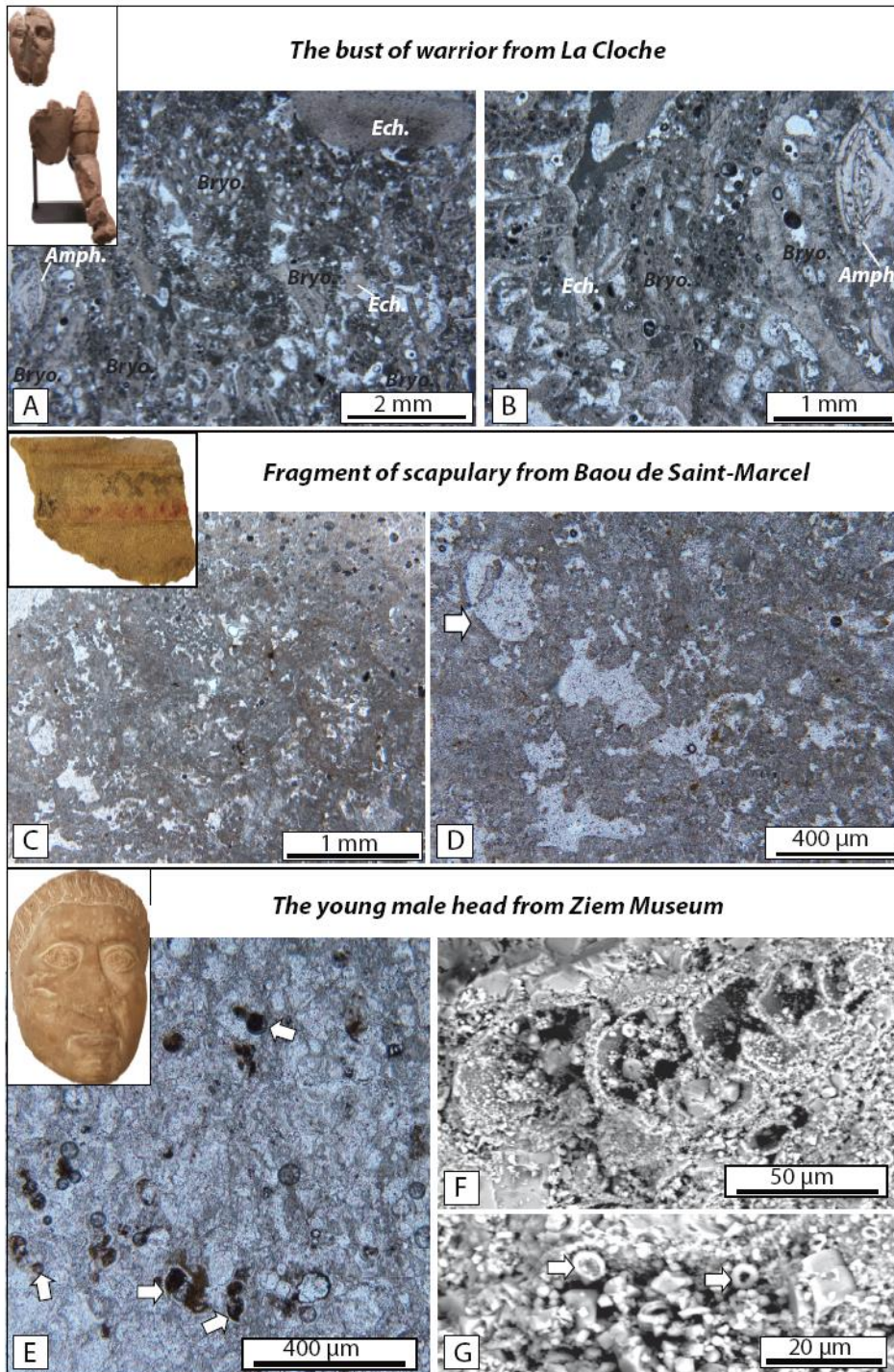


Figure 6: A-B) *Bust of warrior* from La Cloche: thin section microphotograph under polarized light showing the bioclastic packstone-grainstone dominated by bryozoan (Bryo.) and echinoids (Ech.); Amph.: *Amphistegina*; C-D) fragment of scapulary tunic from Baou de Saint-Marcel: thin section microphotograph under polarized light showing the clotted peloidal microfabric; white arrow: calcitic encrustation around plant stem; E-G) The *male head* from Ziem Museum: thin section microphotograph under polarized light showing the planktonic foraminiferal packstone (white arrow: sections of planktonic foraminifers); F) SEM image of a section of *Heterohelix*; G) SEM image showing fragmented coccoliths (white arrow) within the micrite matrix.

FIGURE 7

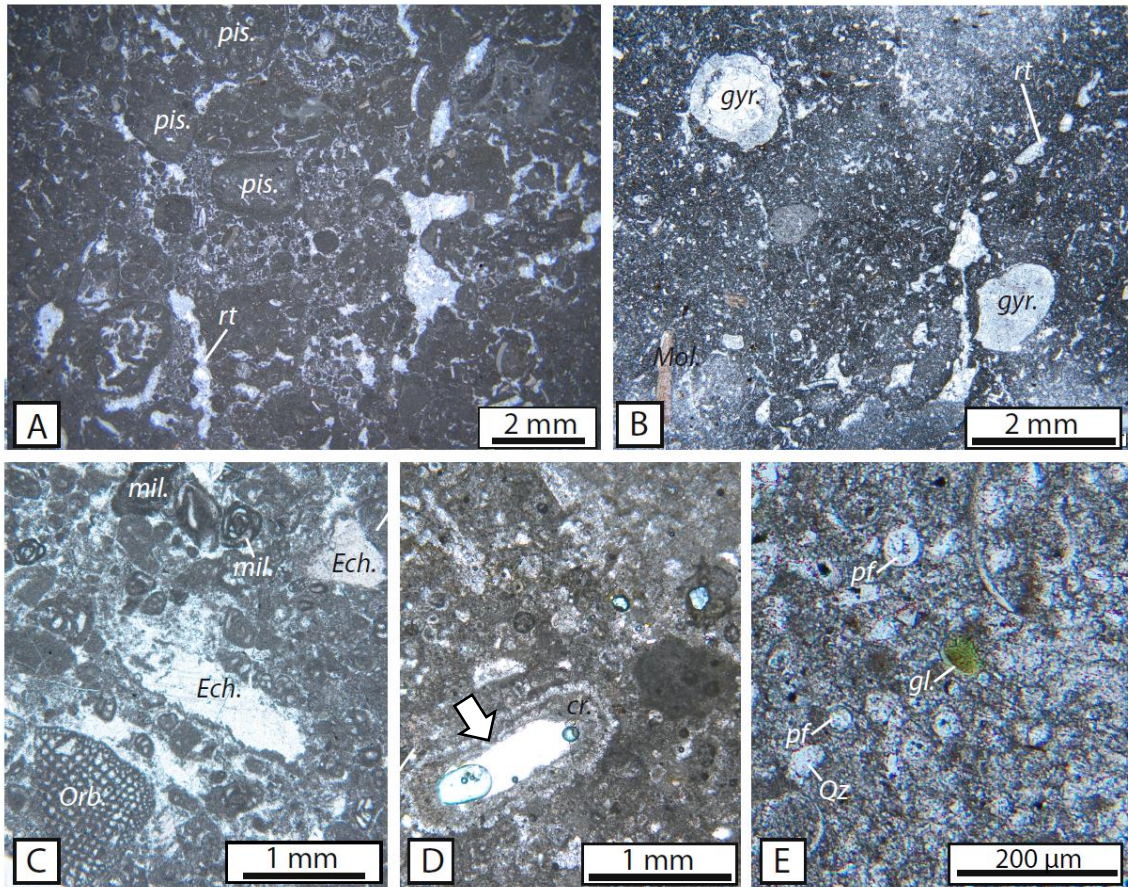


Figure 7: Thin section microphotograph under polarized light of outcrop samples: **A)** local limestone from Roquepertuse oppidum (“Calcaire de Rognac” formation, latest Campanian to earliest Maastrichtian); *rt*: root traces, *pis.*: vadose pisoids; **B)** local limestone from Castellás oppidum (“Calcaire de Rognac”, latest Campanian to earliest Maastrichtian), *gyr.*: characean gyrogonite, *rt*: root traces; **C)** local limestone from La Cloche oppidum (Barremian, Urgonian facies), *Orb.*: orbitolinid, *mil.*: miliolids; *Ech.*: echinoderms; **D)** local limestone from Baou Saint-Marcel oppidum, calcareous tufa (early Pleistocene) with calcite encrustations around stems (arrow), **E)** Planktonic-dominated packstone from the Collongues slump, north-east of Cassis (Fontblanche 2 formation, latest Cenomanian), *pf*: planktonic foraminifer, *Qz*: quartz grain, *gl.*: glauconite.

FIGURE 8

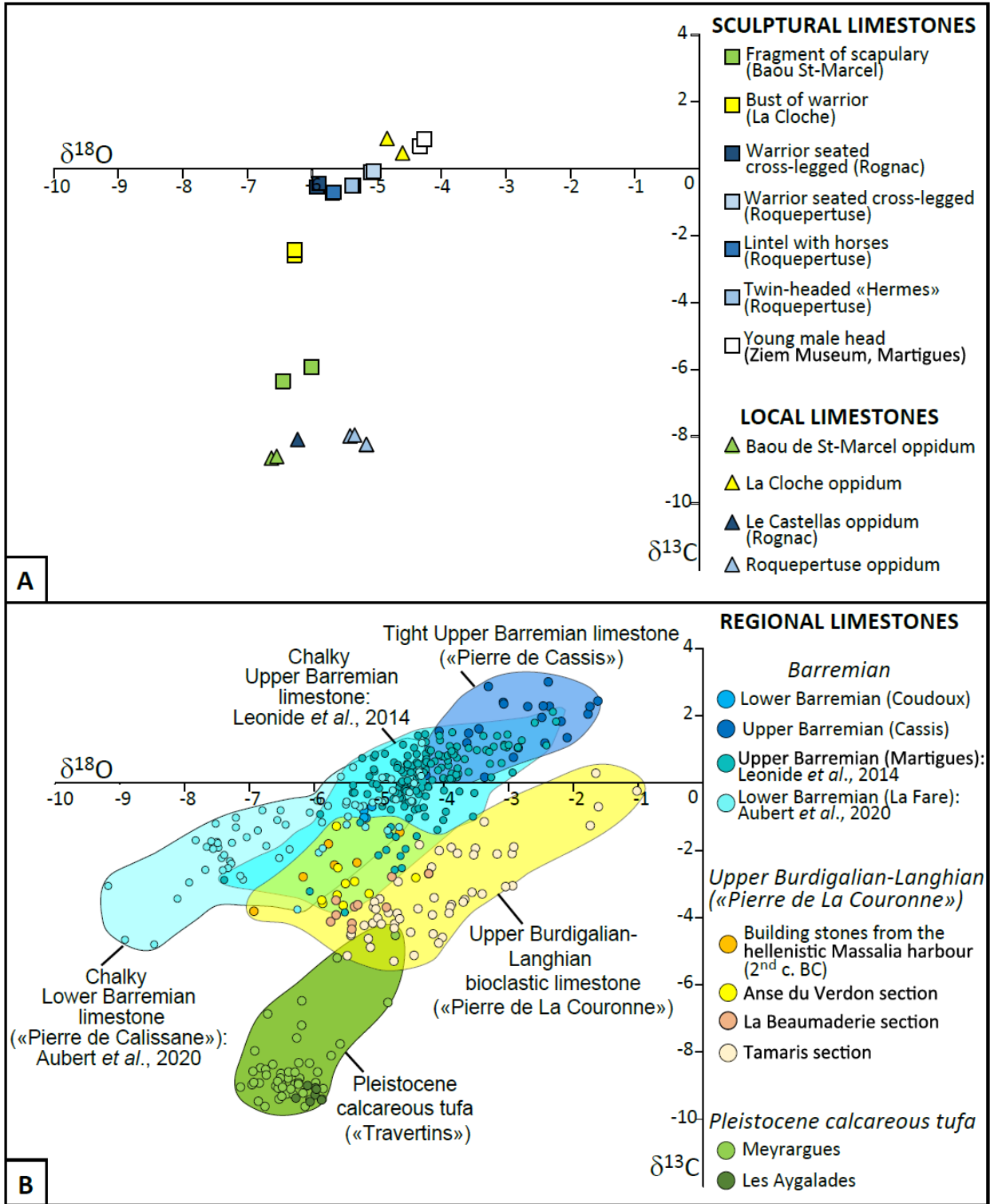


Figure 8: **A)** $\delta^{13}\text{C}$ - $\delta^{18}\text{O}$ cross-plot for sculptural and local limestones, **B)** $\delta^{13}\text{C}$ - $\delta^{18}\text{O}$ cross-plot for the regional limestone database.

FIGURE 9

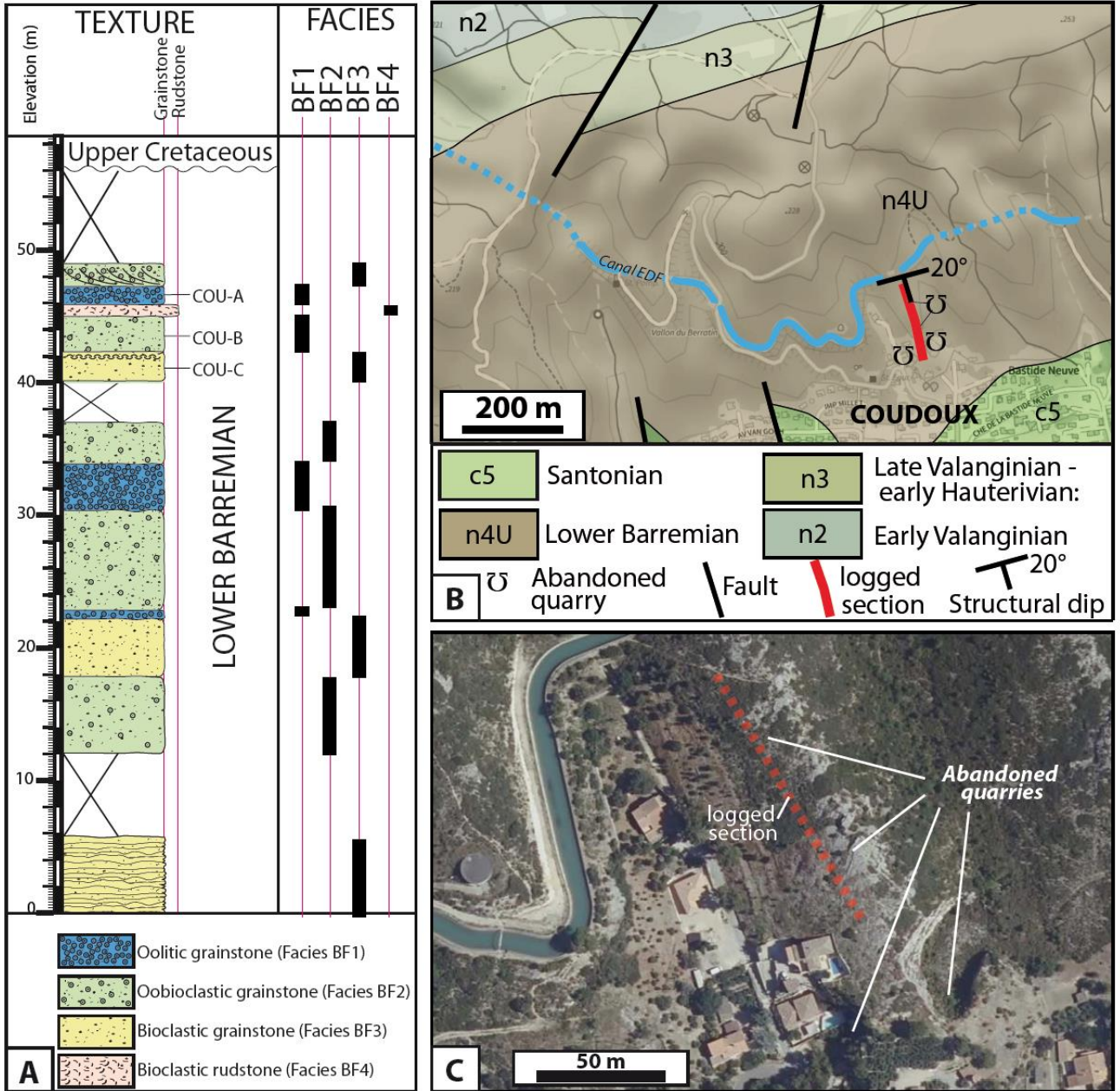


Figure 9: A) Textural log and vertical facies changes of the upper part of Lower Barremian succession, north of Coudoux (see location in B and C); B) Geological map of the southern flank of La Fare Massif, north of Coudoux and position of the section logged in A; C) Aerial view of the logged section and position of abandoned quarries.

FIGURE 10

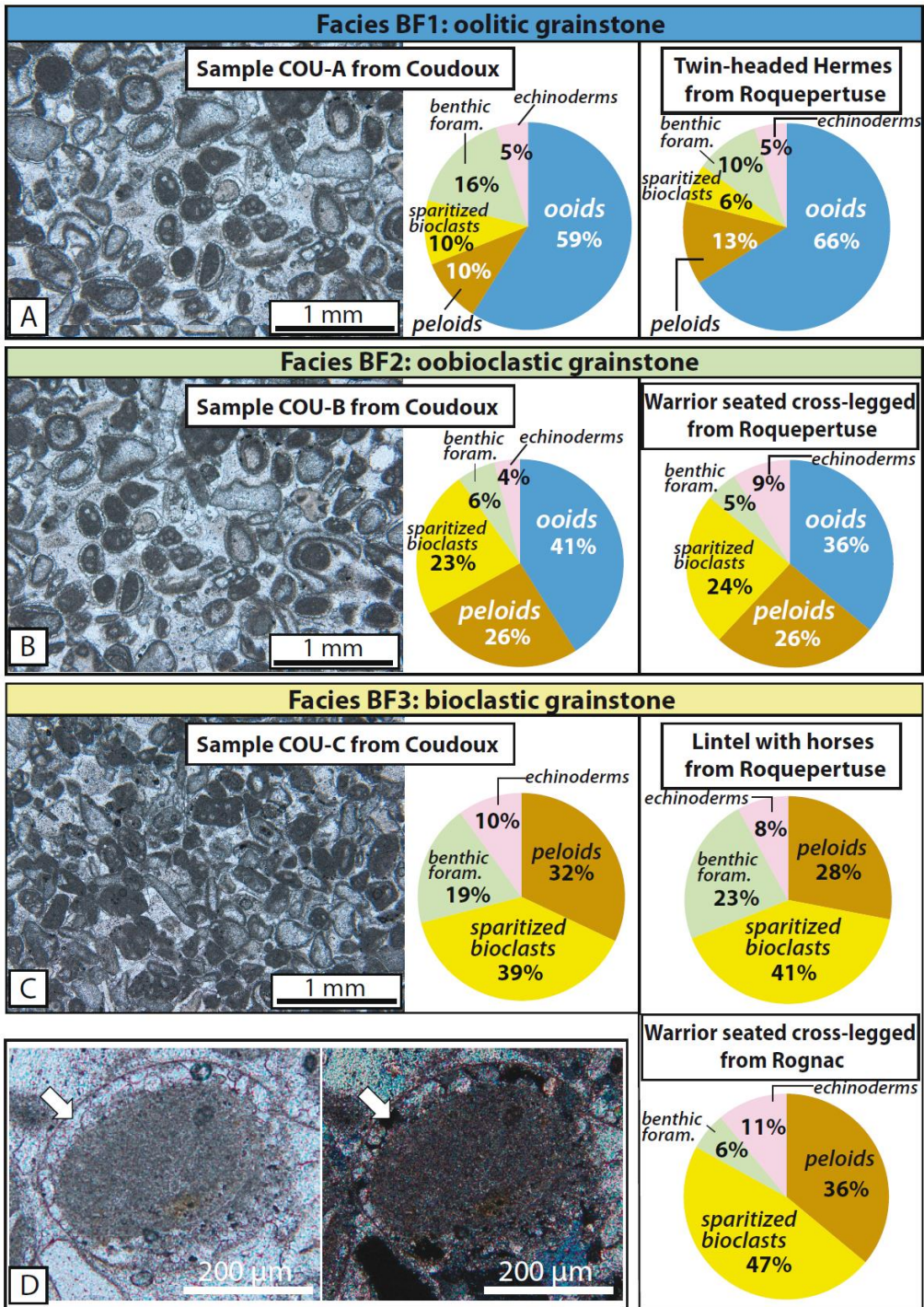


Figure 10: A) Thin section microphotograph of sample COU-A from Coudoux section, showing the oolitic grainstone facies (BF1) and comparison of carbonate grain composition between COU-A and the *twin-headed Hermes* from Roquepertuse; B) Thin section microphotograph of sample COU-B from Coudoux section, showing the oobioclastic grainstone facies (BF2) and comparison of carbonate grain composition between COU-B and the *warrior seated cross-legged* from Roquepertuse; C) Thin section microphotograph of sample COU-C from Coudoux section, showing the bioclastic grainstone facies (BF1) and comparison of carbonate grain composition between COU-A, the *lintel with horses* from Roquepertuse and the *warrior seated cross-legged* from Rognac; D) Detail of an ooid with leached cortex and equigranular sparry calcite infill, under polarized (left) and polarized-analyzed light (right), COU-A sample, Coudoux.

FIGURE 11

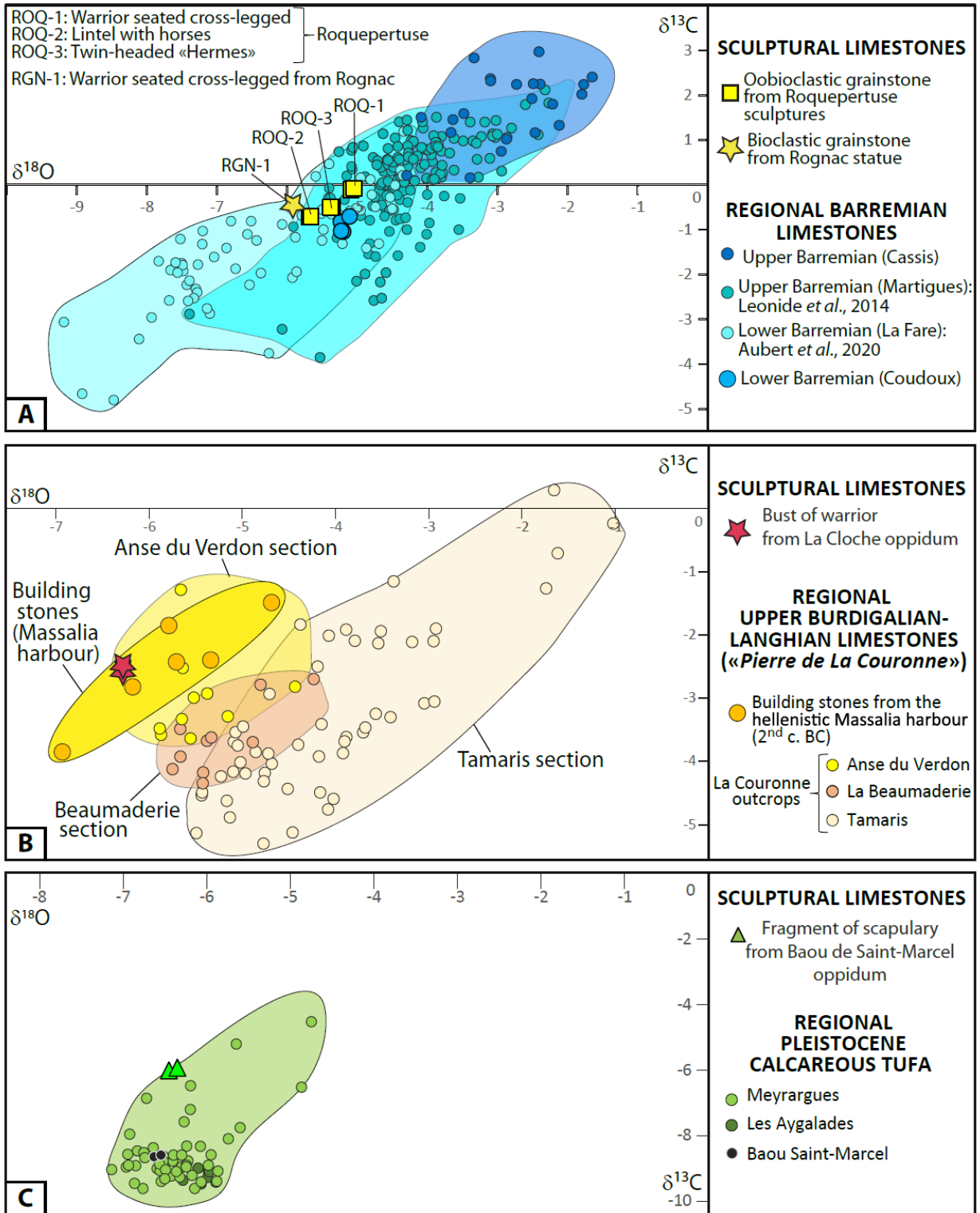


Figure 11: $\delta^{13}\text{C}$ - $\delta^{18}\text{O}$ cross-plots: **A)** Sculptural limestones from Roquepertuse and Rognac and regional Barremian limestones; **B)** Bust of warrior from La Cloche and regional Burdigalian-early Langhian (?) limestones (“Pierre de la Couronne”); **C)** Fragment of scapular tunic from Baou Saint-Marcel and regional Pleistocene calcareous tufa.

FIGURE 12

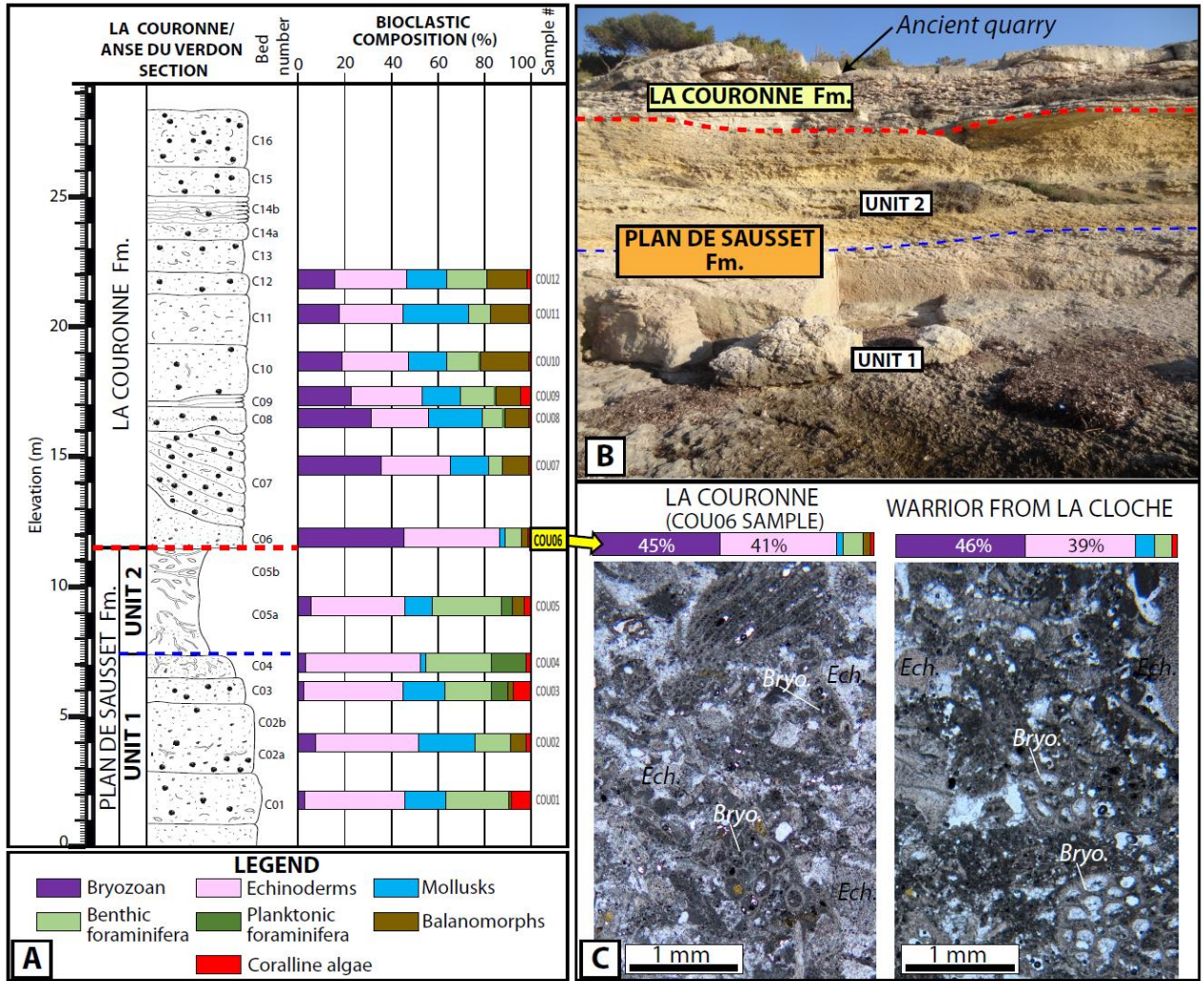


Fig.12: A) Log section of La Couronne/Anse du Verdon (see location in **Fig. 1B**) and bioclastic composition of limestones determined from point counting on thin-section; **B)** Photograph of the outcrop (eastern coast of Anse du Verdon) showing the upward transition from Plan de Sausset (Middle Burdigalian) and La Couronne (Upper-Burdigalian-early Langhian?) formation and the position of ancient quarries on top; **C)** Comparison of microfacies and grain composition between COU6 sample from La Couronne and the *bust of warrior* from La Cloche; Bryo: bryozoan; Ech.: echinoderms.

TABLE 1

<i>Statuary limestone database</i>	Number of thin-sections
Twin-headed Hermes (Roquepertuse): ROQ-3	1
Lintel with horses (Roquepertuse): ROQ-2	1
Warrior seated cross-legged (Roquepertuse): ROQ-1	1
Warrior seated cross-legged (Rognac): RGN-1	1
Bust of warrior (La Cloche); CL-1	1
Fragment of scapulary tunic (Baou de Saint-Marcel): BSM-1	1
Male head (Ziem Museum); ZM-1	1
<i>Local limestones</i>	
Roquepertuse oppidum	3
Le Castellas oppidum	3
La Cloche oppidum	2
Baou Saint-Marcel	2
<i>Regional limestones</i>	
Lower Barremian limestones from La Fare Massif	>200
Upper Barremian limestones from Martigues	50
Cenomanian limestones from Le Beausset bassin	50
La Couronne limestone (Burdigalian-Langhian)	69
Pleistocene calcareous tufa from Provence	30
<i>Building stone limestones (Hellenistic harbor of Massalia)</i>	
Western edge of the freshwater basin (2nd c. BC): MJV3	1
Western quay of the harbour horn: MJV4 (1st c. AD)	1
Interior facing of the south tower (2nd c. BC): MJV5	1
Paving of the freshwater basin (2nd c. BC): MJV6-7	2

Table 1: Thin-section database of limestones from Provence

TABLE 2

	Number of C and O stable isotope measurements
<i>Statuary limestone database</i>	
Twin-headed Hermes (Roquepertuse): ROQ-3	2
Lintel with horses (Roquepertuse): ROQ-2	2
Warrior seated cross-legged (Roquepertuse): ROQ-1	2
Warrior seated cross-legged (Rognac): RGN-1	2
Bust of warrior (La Cloche); CL-1	2
Fragment of scapulary tunic (Baou de Saint-Marcel): BSM-1	2
Male head (Ziem Museum): ZM-1	2
<i>Local limestones</i>	
Roquepertuse oppidum	4
Le Castellas oppidum	1
La Cloche oppidum	2
Baou Saint-Marcel	2
<i>Regional limestones</i>	
Lower Barremian limestones from Cassis ("Cassis Limestone")	22
Lower Barremian limestones from La Fare Massif (Aubert et al., 2020)	66
Upper Barremian limestones from Martigues (Léonide et al., 2014)	163
La Couronne limestone (Burdigalian-Langhian)	78
Pleistocene calcareous tufa from Provence	56
<i>Building stone limestones (Hellenistic harbor of Massalia)</i>	
Western edge of the freshwater basin (2nd c. BC): MJV3	1
Western quay of the harbour horn: MJV4 (1st c. AD)	1
interior facing of the south tower (2nd c. BC): MJV5	1
paving of the freshwater basin (2nd c. BC): MJV6-7	2

Table 2: Carbon and oxygen isotope database of selected limestones from Provence.

TABLE 3

	MgO/ CaO	Al ₂ O ₃ / CaO	SiO ₂ / CaO	Fe/Ca	K/Ca	density (10 ³ kg/m ³)	porosity (%)	P-wave velocity (m/s)
Young Male Head (Ziem Museum)	120	48	96	4	14	2.37	12.6	5032
Roquepertuse: seated warrior (ROQ 1)	90	70	150	9	17			4574
Roquepertuse: lintel with horses (ROQ 2)	160	63	150	7	14			2595
Roquepertuse: Twin- headed Hermes (ROQ 3)	170	46	300	9	20	2.24	17.5	1978
La Cloche: Bust of Warrior (CL1)	140	47	180	5	15	2.16±0.06	20.4 ±2.1	4166
Rognac: seated warrior (RGN1)	240	nd	32	3	11			2558
Coudoux outcrop: COU A	130	17	13	0.4	9	2.56	5.6	
Coudoux outcrop: COU B	160	18	13	0.5	9	2.24	17.3	
Coudoux outcrop: COU C	110	19	15	0.4	10	2.49	7.8	
Roquepertuse outcrop: ROQ C	140	23	18	2	9	2.32	14.3	
Roquepertuse outcrop: ROQ D	110	17	19	2	10	2.4	11.3	
La Cloche outcrop (CLA)	110	19	15	0.3	9			
Rognac-Le Castellas outcrop (RGNA)	nd	23	24	3	10	2.67	1.5	
Mauribas, near Velaux outcrop (MAU A)	90	22	16	4	9	2.41	11	
Baou Tailla (La Couronne)	nd	23	54	9	1.5	2.16	20.4	

Table 3: Results of non-destructive methods: pXRF measurements, density and porosity estimates and P-wave velocity.

APPENDIX

Carbon and oxygen isotope measurements

	Sample identifier	d18O vs PDB (‰)	d13C vs PDB ‰
STATUARY LIMESTONES			
	BSM	-6,45	-6,01
	BSM	-6,35	-5,93
	CL 1	-6,28	-2,58
	CL 1	-6,27	-2,44
	RGN 1	-5,93	-0,55
	RGN 1	-5,89	-0,44
	ROQ 1	-5,09	-0,10
	ROQ 1	-5,05	-0,07
	ROQ 2	-5,68	-0,71
	ROQ 2	-5,66	-0,70
	ROQ 3	-5,36	-0,50
	ROQ 3	-5,38	-0,50
	ZIEM	-4,33	0,68
	ZIEM	-4,26	0,88
LOCAL LIMESTONES			
	BSM A	-6,63	-8,65
	BSM A	-6,55	-8,60
	CL A	-4,60	0,47
	CL A	-4,84	0,91
	RGN A	-6,23	-8,09
	ROQ C	-5,41	-7,98
	ROQ C	-5,34	-7,96
	ROQ D	-5,16	-8,25
	ROQ D	-5,16	-8,23
REGIONAL LIMESTONES			
Lower Barremian limestone, Coudoux			
	COUA	-5,23	-0,82
	COUA	-5,11	-0,70
	COUB	-5,20	-1,04
	COUB	-5,23	-1,03

Upper Barremian limestone, Cassis ("Pierre de Cassis")

CAS-1	-1,78	2,05
CAS-2	-1,75	2,27
CAS-3	-2,49	1,95
CAS-4	-2,37	2,28
CAS-5	-3,08	2,40
CAS-6	-2,47	2,29
CAS-7	-3,31	2,87
CAS-8	-2,39	3,01
CAS-9	-3,62	1,48
CAS-10	-4,28	0,23
CAS-11	-4,07	1,54
CAS-12	-1,63	2,44
CAS-13	-2,71	2,27
CAS-14	-3,46	1,62
CAS-15	-3,37	0,17
CAS-16	-3,08	2,35
CAS-17	-2,44	1,19
CAS-18	-2,10	1,35
CAS-19	-3,64	1,19
CAS-20	-2,85	1,04
CAS-21	-2,93	0,77
CAS-22	-2,19	1,83

"Pierre de La Couronne" (Burdigalian-Langhian)

Building stones: hellenistic Massalia harbour (2nd c. BC)

MJV 2	-4,68	-1,46
MJV 3	-5,34	-2,37
MJV 4	-6,93	-3,81
MJV 5	-6,17	-2,79
MJV 6	-5,69	-2,44
MJV 7	-5,78	-1,81

Tamaris section

TP 01	-5,13	-4,89
TP 02	-5,16	-4,62
TP 03	-4,72	-3,87
TP 04	-4,76	-4,18
TP 05	-3,88	-3,61
TP 05-OR	-2,94	-3,05
TP 06	-4,77	-4,31
TP 06-OR	-5,44	-4,54
TP 07	-4,51	-4,44
TP 07-OR	-5,49	-5,13
TP 08	-4,18	-3,92
TP 08-OR	-3,68	-3,46
TP 09	-4,68	-4,04
TP 09-OR	-5,23	-4,24
TP 10	-5,10	-4,16
TP 10-OR	-5,43	-4,49
TP 11	-4,40	-3,74
TP 12	-3,05	-3,08
TP 13	-2,95	-2,10
TP 13-OR	-1,62	-0,70
TP 14	-1,74	-1,26
TP 14-OR	-1,66	0,29
TP 15	-3,41	-3,30
TP 16	-3,57	-3,25
TP 17	-3,90	-3,68
TP 18	-3,18	-2,11
TP 19	-3,70	-3,54
TP 20	-4,02	-4,59
TP 21	-4,46	-5,12
TP 22	-4,08	-4,76
TP 23	-3,89	-1,91
TP 23-OR	-3,38	-1,15
TP 24	-4,07	-2,01
TP 24-OR	-4,38	-1,84
TP 25	-3,51	-1,94
TP 26	-3,54	-2,13
TP 26-OR	-4,19	-2,50
TP 27	-3,79	-2,09
TP 28	-3,92	-3,87
TP 29	-4,17	-4,49

TP 30	-2,92	-1,90
TP 30-OR	-1,02	-0,24
TP 31	-4,15	-3,41
TP 32	-4,77	-5,30
TP 33	-5,09	-3,69
TP 33-OR	-4,99	-3,45
TP 34	-5,07	-3,54
TP 34-OR	-4,71	-2,93
TP 35	-4,86	-3,85
TP 36	-5,05	-3,75
TP 37	-5,02	-4,01
TP 38	-4,97	-4,19

Beaumaderie section

BP 01	-4,89	-3,69
BP 01 OR	-5,67	-3,49
BP 02	-5,75	-4,12
BP 02 OR	-5,42	-4,18
BP 03	-5,66	-3,92
BP 03 OR	-5,42	-4,35
BP 04	-5,38	-3,67
BP 04 OR	-5,33	-3,62
BP 05	-4,80	-2,79
BP 05 OR	-4,23	-2,70

Anse du Verdon section

V 01	-5,87	-3,58
V 01 OR	-5,55	-3,64
V 02	-5,89	-3,48
V 02 OR	-5,65	-3,33
V 03	-5,15	-3,29
V 03 OR	-5,52	-2,99
V 04	-5,64	-2,52
V 04 OR	-5,66	-1,29
V 05	-5,38	-2,93
V 05 OR	-4,43	-2,82

Calcareous tuffa from Provence (Pleistocene)

Meyrargues

M 8	-6,24	-8,32
M 9	-6,22	-8,77
M 10	-6,52	-8,64
M 11	-6,51	-8,94
M 12	-5,95	-8,59
M 13-A	-6,41	-8,78
M 13-B	-6,30	-8,95
M 19	-6,08	-8,33
M 18	-6,96	-8,97
M 27	-5,86	-9,08
M 38	-6,43	-9,24
M 39	-6,59	-9,01
M 40-A	-6,52	-8,77
M 41	-5,98	-8,91

M 42	-6,17	-9,22
M 43	-5,74	-8,10
M 44-A	-6,24	-8,91
M 14-A	-6,72	-6,86
M 14-B	-6,19	-6,48
M 15-A	-6,83	-8,47
M 15-B	-6,94	-8,57
M 16-A	-4,86	-6,52
M 16-B	-5,65	-5,20
M 17	-7,14	-9,04
M 29-A	-5,88	-9,40
M 30	-6,32	-9,27
M 34	-6,56	-9,07
M 1	-6,20	-7,21
M 2	-6,64	-8,37
M 3-4	-6,40	-8,59
M 3-B	-6,75	-8,52
M 4	-5,60	-7,76
M 5	-6,56	-8,87
M 6	-6,54	-9,40
M 7	-6,30	-8,60
M 20	-6,36	-9,10
M 21	-6,74	-8,68
M 22	-6,85	-8,92
M 23	-4,75	-4,53
M 24	-6,49	-9,04
M 25	-6,24	-8,95
M 26	-6,50	-9,32
M 28	-6,76	-9,61
M 31	-6,14	-9,61
M 32	-6,93	-8,90
M 33	-6,07	-9,42
M 35	-6,92	-7,96
M 36	-6,27	-7,58
M 37	-6,86	-9,46

Les Aygalades

A1a	-5,99	-9,28
A1b	-6,28	-9,37
A2	-6,06	-9,47
A3	-5,98	-9,06
A5	-6,10	-8,99
A6	-5,89	-9,42
A7	-5,97	-9,10